Лаборатория мезонной физики
ОФВЭ ПИЯФ им.Б.П.Константинова

Отчет за 2012 год
о ходе выполнения научно-исследовательской работы
«Барионная спектроскопия и физика с η-мезонами.»

Зав. лабораторией В.В.Сумачёв.

ЛМФ2012 (пион-нуклон)+(гамма-нуклон)

В 2012 году сотрудники Лаборатории мезонной физики ОФВЭ участвовали в исследованиях на пионном пучке синхроциклотрона ПИЯФ, обработке данных, полученных на пионном пучке ускорителя ИТЭФ и в экспериментах на пучках фотонов ускорителей ELSA (Bonn) и MAMI-C (Mainz).

Выполненный этап в ПИЯФ в 2012 году:

Завершена обработка результатов экспериментов на СЦ ПИЯФ по измерению сечений реакции $\pi^- p \to \eta n$ в около пороговой области импульсов (до 730 МэВ/с). Результаты приняты к публикации в журнале «Ядерная физика».

Частично набрана статистика при импульсе 740 МэВ/с.

В рамках программы исследования процесса рождения η-мезона на π-мезонном канале синхроциклотрона ПИЯФ выполнены с помощью спектрометра нейтральных мезонов измерения дифференциальных сечений реакции $\pi^- p \to \eta n$ при импульсах налетающих пионов вблизи порога этой реакции, который составляет 685 МэВ/с. Форма дифференциальных сечений, полученных при указанных импульсах, различается весьма существенно – если при 700 МэВ/с сечения практически изотропны по углу, то при 710, 720 и 730 МэВ/с угловая зависимость анизотропна, но симметрична относительно $\cos\theta_{cm} = 0$ (напоминает профиль тарелки). Всё это говорит о том, что если непосредственно вблизи порога процесс $\pi^- p \to \eta n$ идёт преимущественно через образование резонанса S11(1535) с его последующим распадом по каналу ηN, то при более высоких импульсах заметно проявляется D-волна, в то время как P-волна практически отсутствует.

Систематические ошибки измерений не превышают $\pm 5\%$

Основной принцип спектрометра – определение полной энергии образовавшегося η-мезона E_η и угла θ_η, под которым он образовался , на основе измерения энергий двух фотонов от распада $\eta \to \gamma\gamma$ и углов их вылета. Спектрометр состоит из двух электромагнитных калориметров полного поглощения, каждый из которых представляет собой матрицу из 24 кристаллов CsI(Na).

Калориметры спектрометра расположены таким образом, чтобы в одном эксперименте можно было измерить дифференциальные сечения процесса $\pi^- p \to \eta n$ в угловом диапазоне от 0° до 180° в системе центра масс. Всего в этом диапазоне получено десять статистически обеспеченных значений сечения.

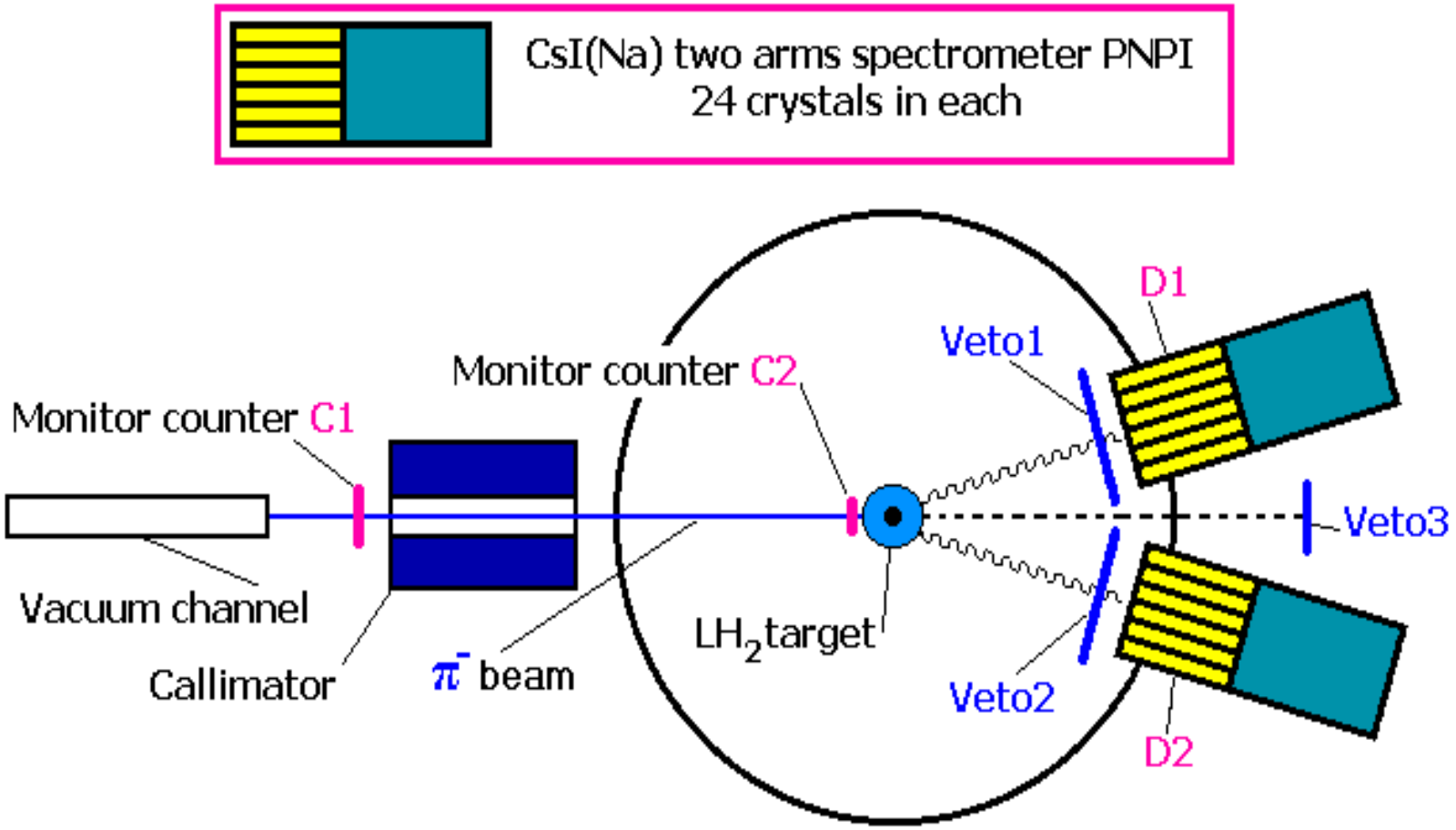

Trigger is C1&C2&D1&D2&$\overline{\text{Veto1}}$&$\overline{\text{Veto2}}$&$\overline{\text{Veto3}}$ for charge exchange reaction

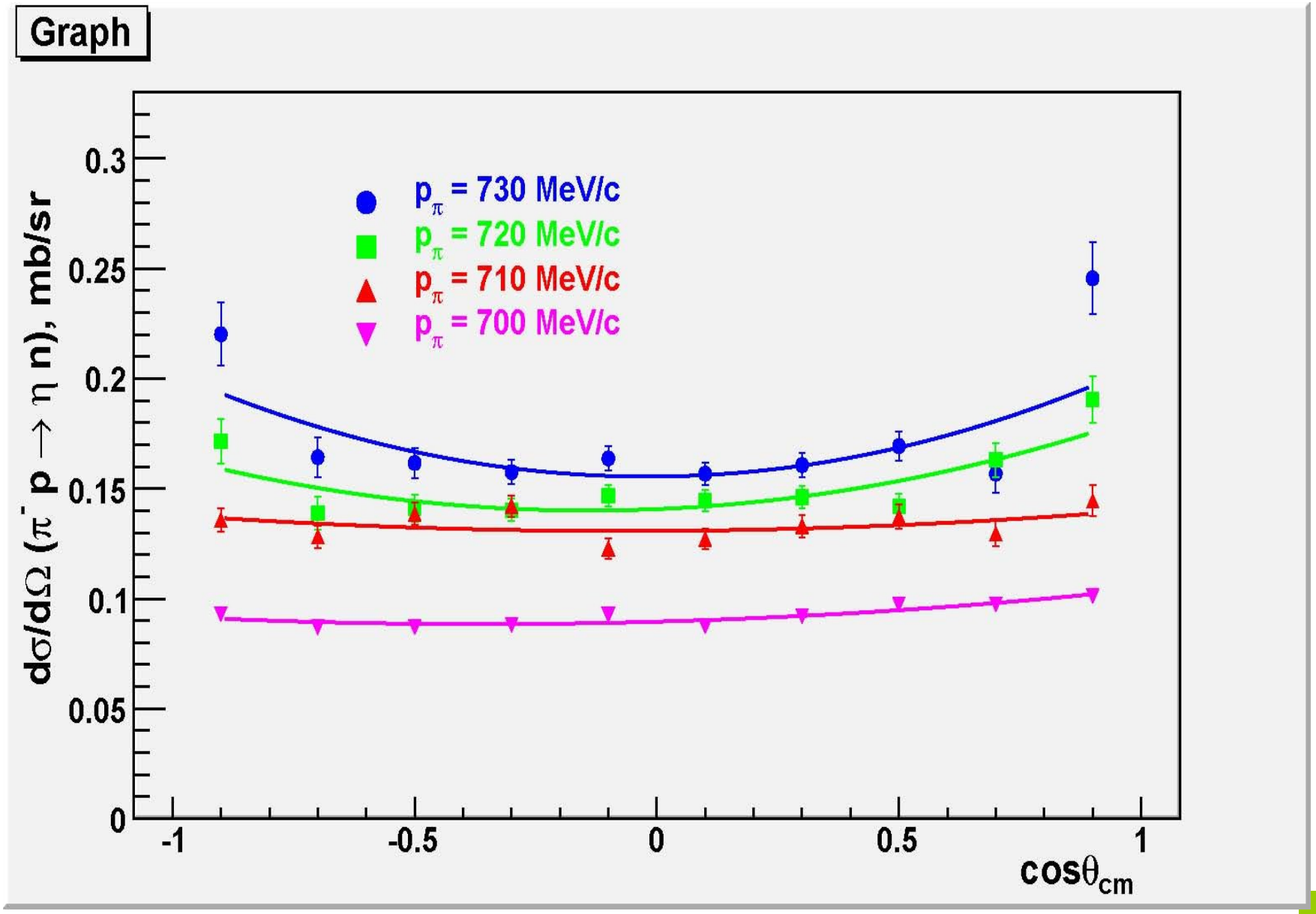
Graph
p_π = 730 MeV/c
p_π = 720 MeV/c
p_π = 710 MeV/c
p_π = 700 MeV/c
$d\sigma/d\Omega\ (\pi^- p \to \eta n)$, mb/sr
0
0.05
0.1
0.15
0.2
0.25
0.3
-1
-0.5
0
0.5
1
$\cos\theta_{cm}$

Дифференциальные (в мбн/ср) и полные (в мбн) сечения реакции $\pi^- p \to \eta n$.

$\cos\theta_\eta^{cm}$	Импульс налетающих пионов, МэВ/c			
	700	710	720	730
– 0.9	0.0953 ± 0.0025	0.0958 ± 0.0027	0.2085 ± 0.0109	0.2561 ± 0.0143
– 0.7	0.0934 ± 0.0027	0.1422 ± 0.0056	0.1483 ± 0.0074	0.1835 ± 0.0090
– 0.5	0.0977 ± 0.0028	0.1494 ± 0.0054	0.1503 ± 0.0062	0.1844 ± 0.0073
– 0.3	0.0997 ± 0.0027	0.1478 ± 0.0050	0.1595 ± 0.0056	0.1819 ± 0.0062
– 0.1	0.1099 ± 0.0029	0.1328 ± 0.0049	0.1601 ± 0.0054	0.1807 ± 0.0061
+ 0.1	0.1002 ± 0.0028	0.1309 ± 0.0047	0.1510 ± 0.0051	0.1747 ± 0.0058
+ 0.3	0.1019 ± 0.0029	0.1406 ± 0.0053	0.1541 ± 0.0054	0.1763 ± 0.0060
+ 0.5	0.1046 ± 0.0030	0.1463 ± 0.0057	0.1581 ± 0.0059	0.1722 ± 0.0066
+ 0.7	0.0982 ± 0.0028	0.1435 ± 0.0063	0.1702 ± 0.0073	0.1954 ± 0.0088
+ 0.9	0.0958 ± 0.0027	0.1568 ± 0.0074	0.2325 ± 0.0111	0.2699 ± 0.0154
	1.253 ± 0.035	1.813 ± 0.071	2.127 ± 0.089	2.482 ± 0.107

Следующий этап программы включает в себя изучение процесса рождения η-мезона на связанном протоне дейтрона $\pi^- d \rightarrow \eta n(n)$ и на связанном нейтроне дейтрона $\pi^+ d \rightarrow \eta p(p)$. Сравнение сечений реакций $\pi^- d \rightarrow \eta n(n)$ и $\pi^+ d \rightarrow \eta p(p)$ может служить хорошим тестом нарушений зарядовой симметрии в процессе рождения η-мезона.

Сначала планируется измерить с помощью спектрометра нейтральных мезонов сечения процесса $\pi^- d \rightarrow \eta nn$ на жидко дейтериевой мишени при том же импульсе 730 МэВ/с, при котором ранее были измерены сечения реакции $\pi^- p \rightarrow \eta n$ на жидководородной мишени. Цель этого этапа – подтвердить, что сечение рождения η-мезона на протоне, связанном в дейтроне, имеет практически ту же величину, что и сечение рождения η-мезона на свободном протоне – естественно, после введения соответствующих поправок на Ферми-движение, принцип Паули и пр.

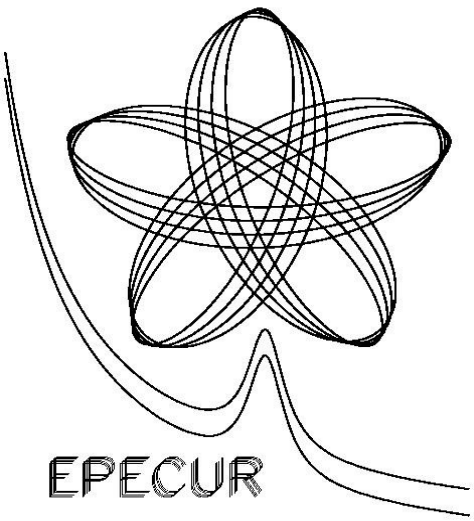

Эксперимент ЭПЕКУР на ускорителе ИТЭФ.

И.Г. Алексеев, И.Г. Бордюжин, Д.В. Калинкин, В.П. Канавец , Л.И. Королева,
Б.В. Морозов, В.М. Нестеров, В.В. Рыльцов, Д.Н. Свирида, П.С. Смирнов,
А.Д. Сулимов, Д.А. Федин, М.М. Шестакова, Б.М. Шурыгин
ИТЭФ, Москва
В.А. Андреев, В.В. Голубев, А.Б. Гриднев, А.И. Ковалев , Н.Г. Козленко, В.С. Козлов,
А.Г. Кривший, В.А. Кузнецов, Д.В. Новинский, В.В. Сумачев, В.И. Тараканов,
В.Ю. Траутман, Е.А. Филимонов
ПИЯФ, Гатчина
M. Sadler
ACU, Abilene, USA

- Установка ЭПЕКУР – первые результаты обработки.

---

*Эксперимент по поиску **ПЕ**нта**К**варка в **У**пругом **Р**ассеянии (и реакции $\pi^- p \to K_S^0 \Lambda$)

PDG 2012- проблема недостающих резонансов

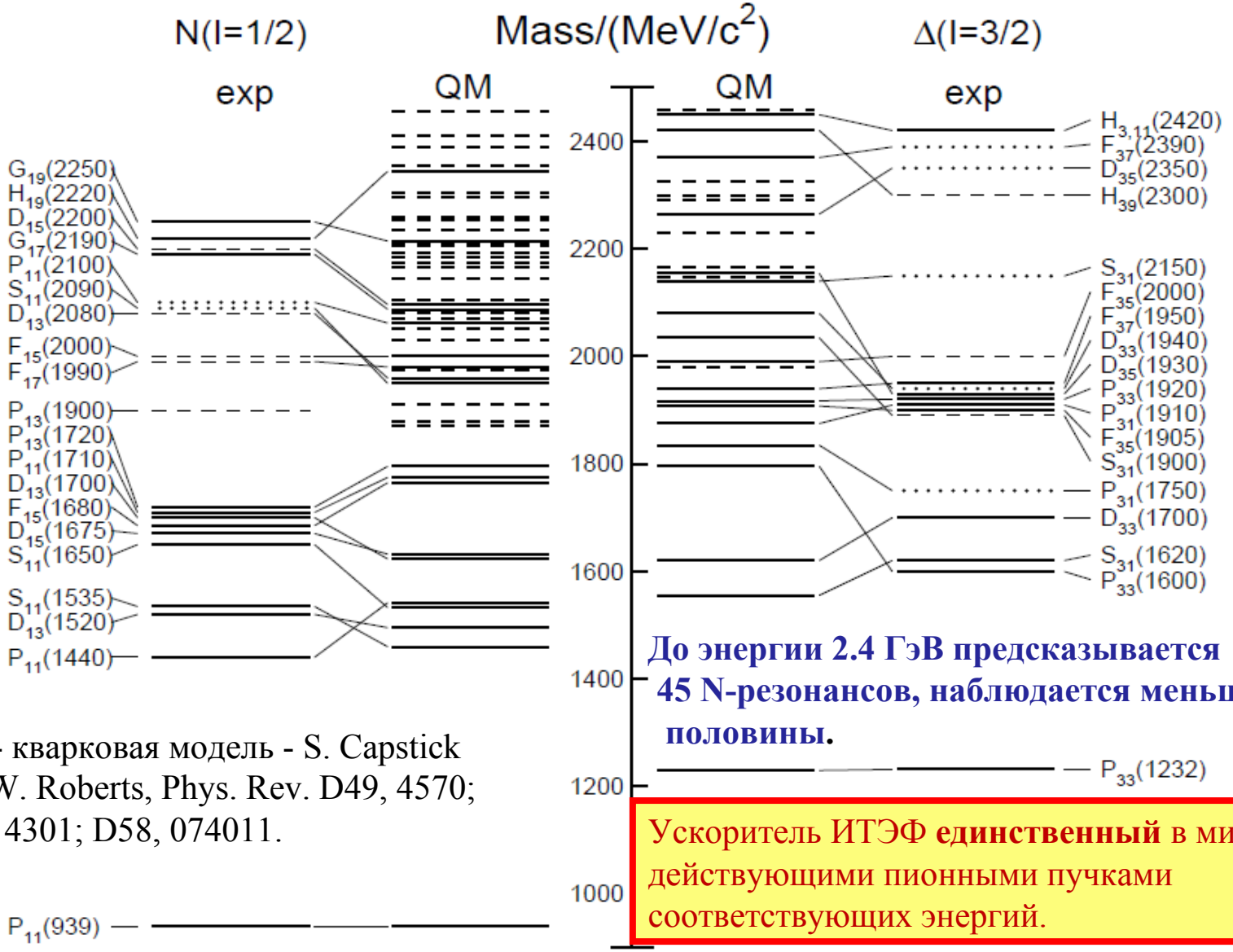

До энергии 2.4 ГэВ предсказывается 45 N-резонансов, наблюдается меньше половины.

QM - кварковая модель - S. Capstick and W. Roberts, Phys. Rev. D49, 4570; D57, 4301; D58, 074011.

Ускоритель ИТЭФ **единственный** в мире с действующими пионными пучками соответствующих энергий.

ЭПЕКУР- Исследование реакций : $\pi^- p \to \pi^- p$ and $\pi^- p \to K^0_S \Lambda$

- "Formation" – type experiment.
- Extremely high invariant mass resolution (~0.6 MeV), provided by high momentum resolution of the magneto-optic channel 0.1%.
- High statistical precision: 0.5% for elastic scattering and 1% for KΛ-production.
- Magnetless spectrometer with drift chambers.
- Liquid hydrogen target.
- Very small amount of matter on the particle paths.

Resonance parameters within safe reach by the experiment:

This provides a good coverage of both theoretical and experimental expectations.

Не только узкие резонансы…

- Precise cross section measurements:

$\pi^- p \to \pi^- p$: $d\sigma/d\Omega$ – 0.5% statistical precision and 1 MeV momentum step

$\pi^- p \to K^0 \Lambda$: σ_{REAC} – 1% statistical precision and the same step

$\Rightarrow$ Very important data for PWA

- Usual resonace P11 N(1710)***
- Λ-polarization in the reaction $\pi^- p \to K^0 \Lambda$ - an order of magnitude better precision then the best data available now - NIMROD (78)

⊙ Proportional chambers with 1mm pitch and 40 um aluminum foil potential electrode in the first focus (1FCH1-4) and in front of the target (2FCH1-4).

⊙ Liquid hydrogen target with beryllium outer shell and mylar hydrogen container. The target diameter is 40 mm and the length along the beam ~250 mm.

⊙ 8 modules of drift chambers with hexagonal structure to measure tracks of particles produced.

⊙ Trigger scintillation counters S1, S2, A1.

⊙ NMR system for measurement field in the magneto-optic channel dipoles with precision better 0.1%.

⊙ Triggers:

Main = S1·1FCH ·S2 ·2FCH ·(!A1)

With prescale:

Mom1F = S1·1FCH ·S2 ·2FCH

BeamPos = S1·1FCH·2FCH · A1

Setup for elastic scattering

$\pi p \rightarrow \pi p$

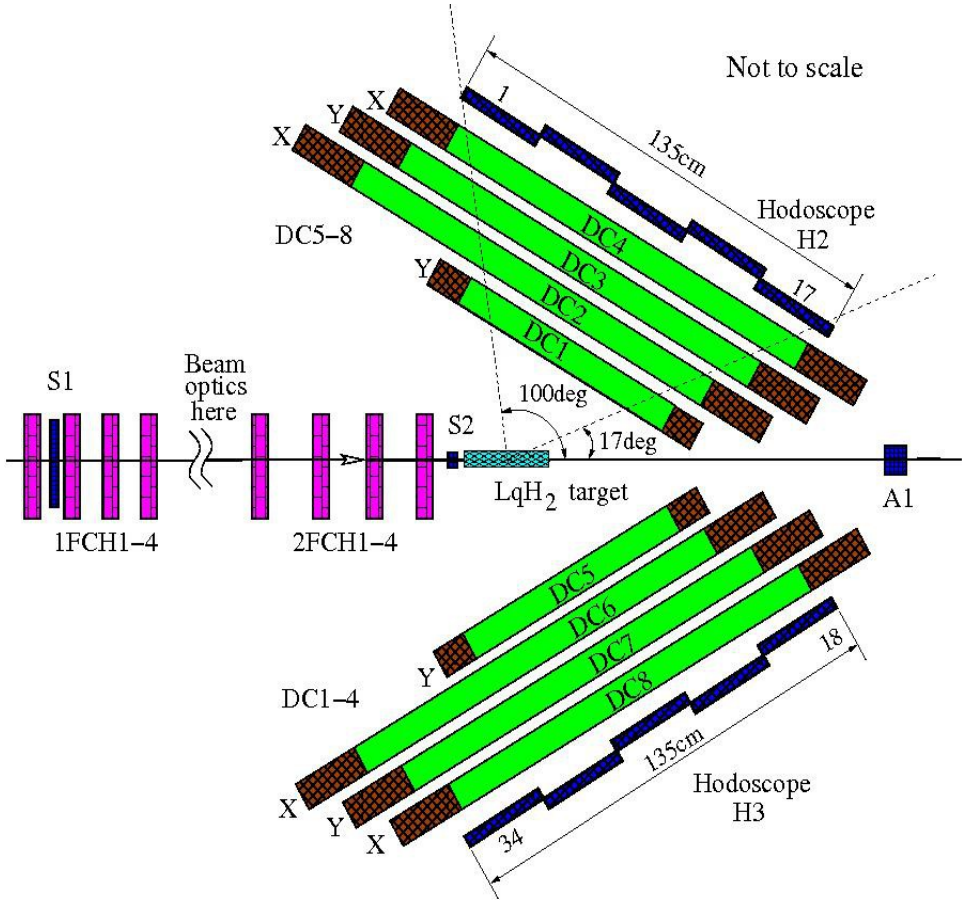

В 2009 – 2011 годах набрана статистика в упругом πN – рассеянии :

π^+p – рассеянии - 0.95млрд. соб.; π^-p – рассеянии – 2.0 млрд.соб.

В 2012 году продолжена обработка ранее набранных событий.

На следующем рисунке представлена часть полученных результатов.

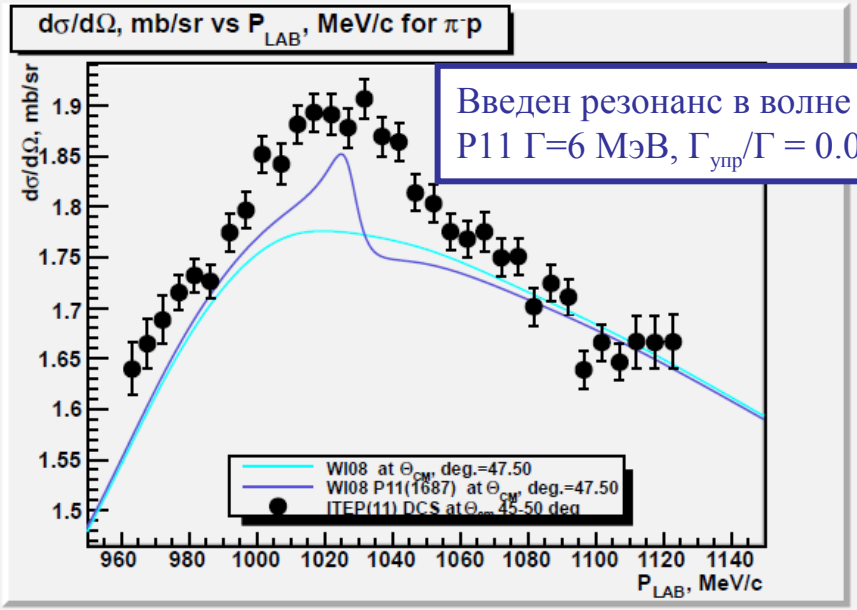

Введен резонанс в волне
P11 Γ=6 МэВ, $\Gamma_{упр}/\Gamma = 0.05$

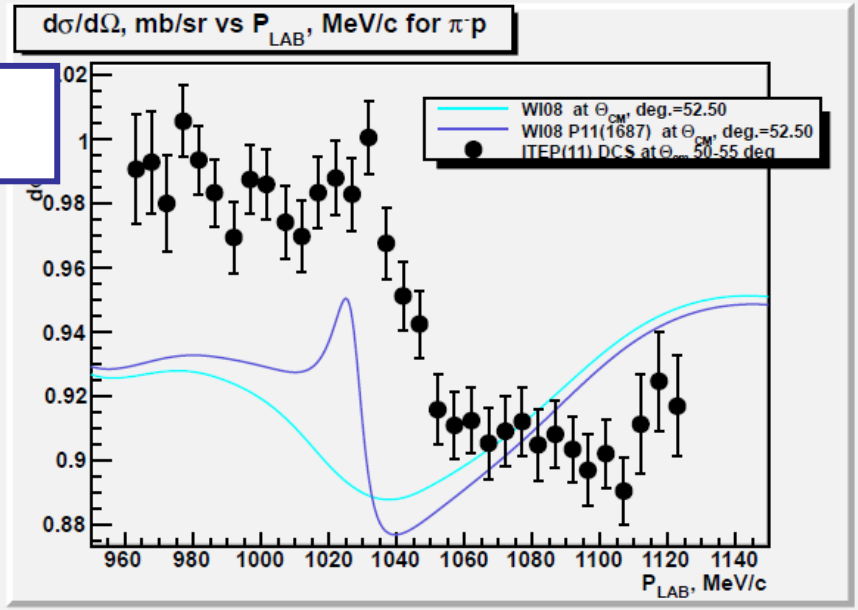

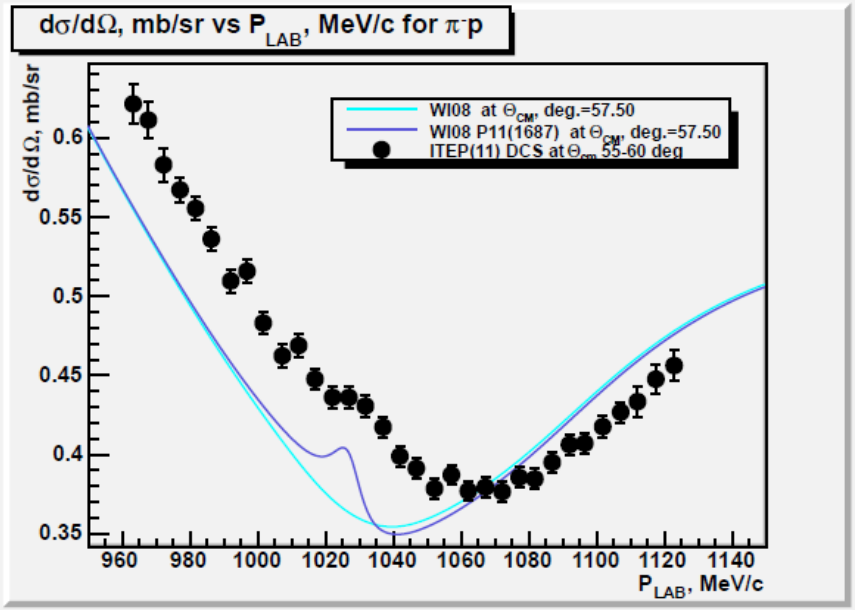

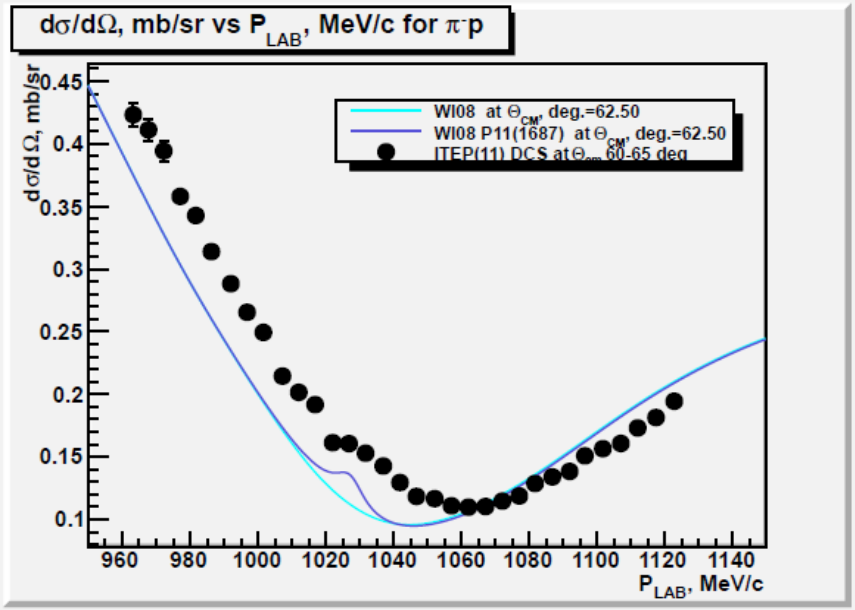

Предварительно

Наблюдается узкая особенность при P_{lab}=1020-1040 МэВ/с. Для выяснения природы и квантовых чисел на март 2012 года был запланирован на пионном пучке ускорителя ИТЭФ набор дополнительной большой статистики в узкой области P_{lab}=1000-1060 МэВ/с.

ЛМФ2012 (ПИОН-НУКЛОН)

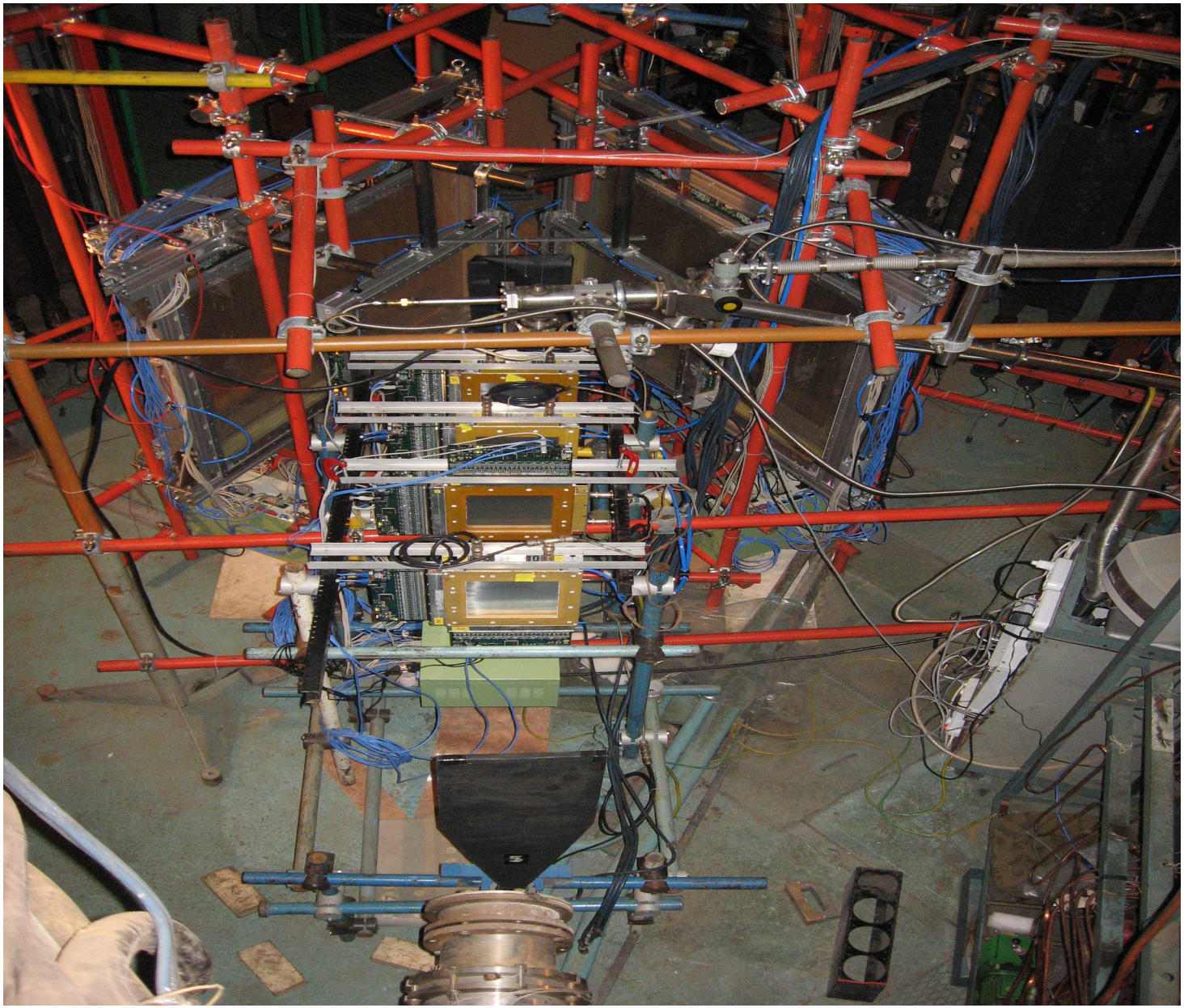

Статус эксперимента «ЭПЕКУР»

- Собрана и запущена установка по прецизионному измерению упругого пион-протонного рассеяния.

Достигнуты:

- ✓ эффективность регистрации треков в дрейфовых камерах – выше 99%.
- ✓ точность измерения импульса частиц пучка не хуже 0.1%
- ✓ качество нормировки не хуже 0.7%

- Набрана статистика 2.95 млрд. событий. Ведется обработка набранной информации, которая будет продолжена в 2013 году.
- Предварительные результаты демонстрируют особенность в области импульсов 1020-1040 МэВ/с.
- Установка практически не пострадала от пожара. Ведется очистка электроники и камер от копоти.

Если переносить эксперимент, то куда?

- Нуклотрон ОИЯИ – нет готового пучка, время работы ускорителя на потребителей – несколько недель в году;
- У70 ИВФЭ – нет готового пучка, время работы ускорителя – 1.5 месяца в году;
- SIS18 GSI – недостаточная энергия (4.5 ГэВ) => недостаточная интенсивность пионного пучка;
- AGS BNL – на 100% задействован как инжектор RHIC, закрыты все fixed-target программы.
- Main Injector synchrotron, Fermilab – можно рассматривать после завершения первой стадии реконструкции в 2016 году.
- JPARK – большая конкуренция за пучки, которые должны быть полностью запущены в 2015 году.
- PS CERN – нет готового пучка.

Ускоритель ИТЭФ – оптимален для нашего эксперимента.

Ускоритель - ELectron Stretcher Anlage (ELSA)

- Energy range 0.5–3.5 GeV
- Max. extracted intensity ∼ 1nA
- Electron polarisation ∼ 60–80%

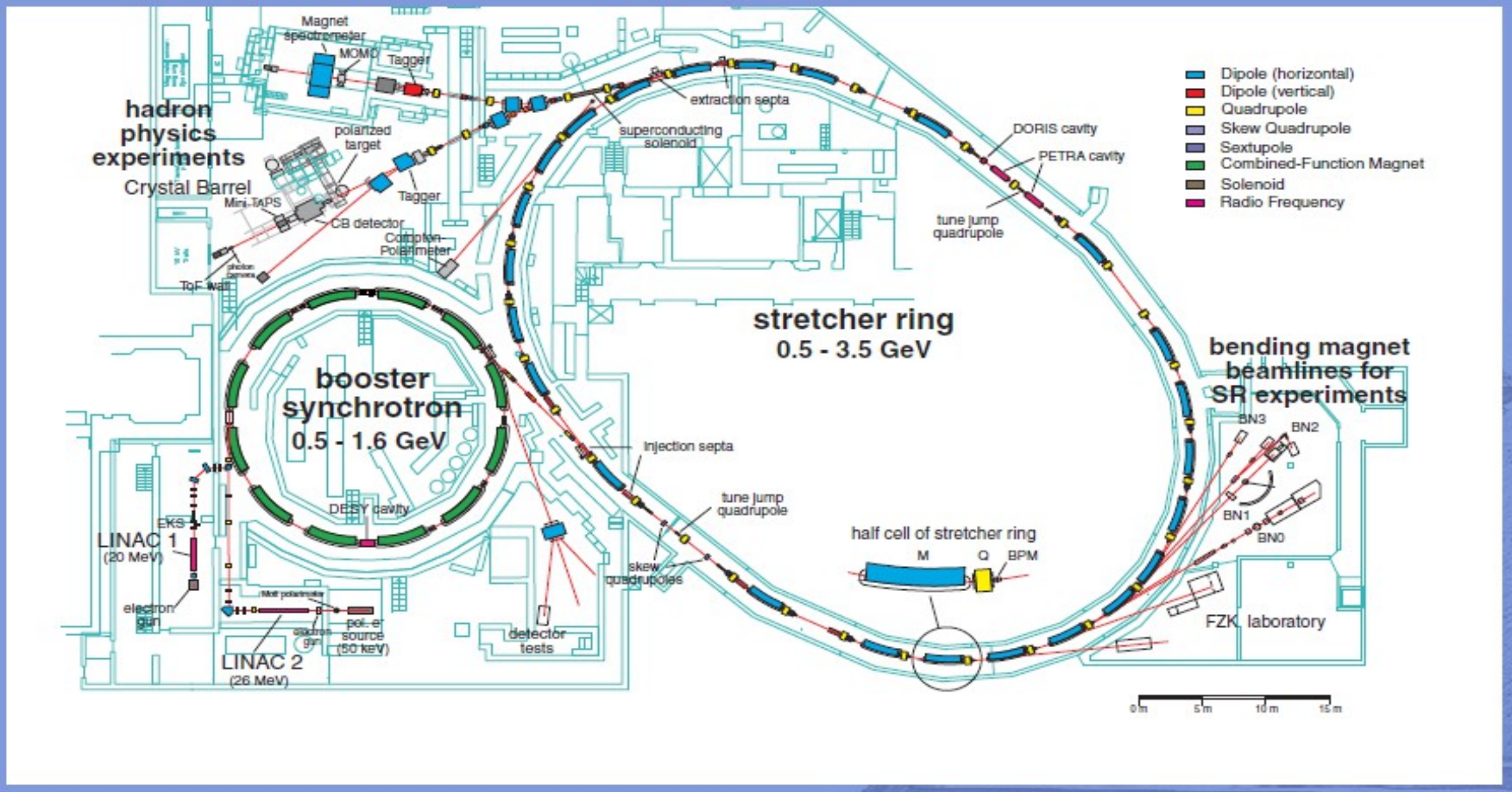

Experimental Setup

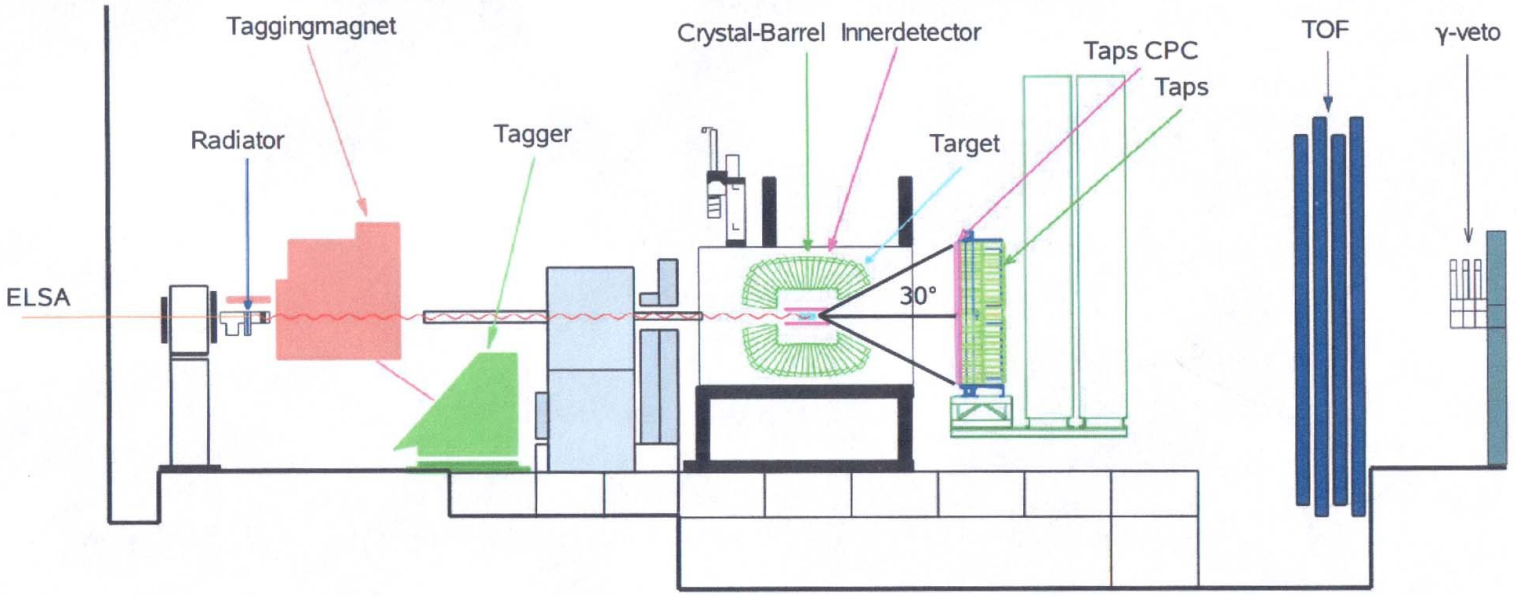

3.3 GeV $E_{electron}$ up to 3GeV photons LH_2/LD_2 1290 CsI crystals 522 BaF crystals

4π geometry, high sensitivity to multiphoton final states

physics aims:

meson production and **baryon spectroscopy**

Схема установки CB-ELSA

universitätbonn

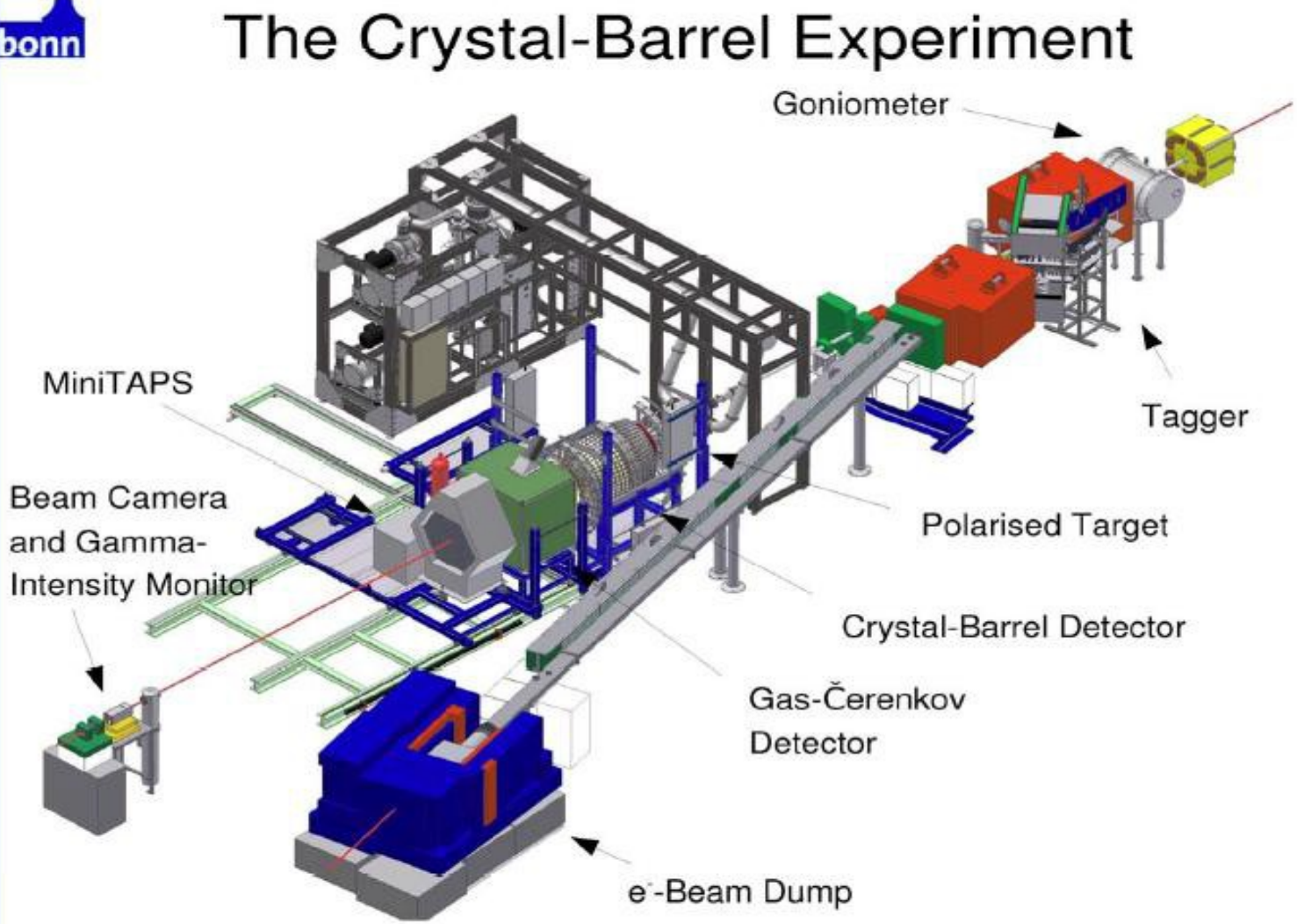

Photon		Target			Recoil			Target–Recoil			
					x'	y'	z'	x'	x'	z'	z'
		x	y	z				x	z	x	z
unpolarized	σ	0	T	0	0	P	0	$T_{x'}$	$-L_{x'}$	$T_{z'}$	$L_{z'}$
linearly	$-\Sigma$	H	$(-P)$	$-G$	$O_{x'}$	$(-T)$	$O_{z'}$	$(-L_{z'})$	$(T_{z'})$	$(-L_{x'})$	$(-T_{x'})$
circularly	0	F	0	$-E$	$C_{x'}$	0	$C_{z'}$	0	0	0	0

- the 4 independent helicity amplitudes of single pseudoscalar meson photoproduction can be uniquely determined by 8 out of 16 accessible observables, among:
  - 4 double polarization observables (at least 2 recoil observables),
  - 2 with transversally polarized target,
- with transversally polarized target, P can be measured without measuring the polarization of the recoil proton
- complete set: Σ, σ, T, P, G, E, C_x, C_z
- C_x, C_z are measured for single π production (Phy. Rev. C66 034614 2002)
  $\rightarrow$ with these measurements a complete experiment is possible

Well-established nucleon resonances revisited by double-polarization measurements.

The first measurement is reported of the double-polarization observable G in photoproduction of neutral pions off protons, covering the photon energy range from 620 to 1120 MeV and the full solid angle. G describes the correlation between the photon polarization plane and the scattering plane for protons polarized along the direction of the incoming photon. The observable is highly sensitive to contributions from baryon resonances. The new results are compared to the predictions from SAID, MAID, and BnGa partial wave analyses. In spite of the long-lasting efforts to understand $\gamma p \to p\pi^0$ as the simplest photoproduction reaction, surprisingly large differences between the new data and the latest predictions are observed which are traced to different contributions of the $N(1535)$ with spin-parity $J^P = 1/2^-$ and $N(1520)$ with $J^P = 3/2^-$. In the third resonance region, where $N(1680)$ with $J^P = 5/2^+$ production dominates, the new data are reasonably close to the predictions.

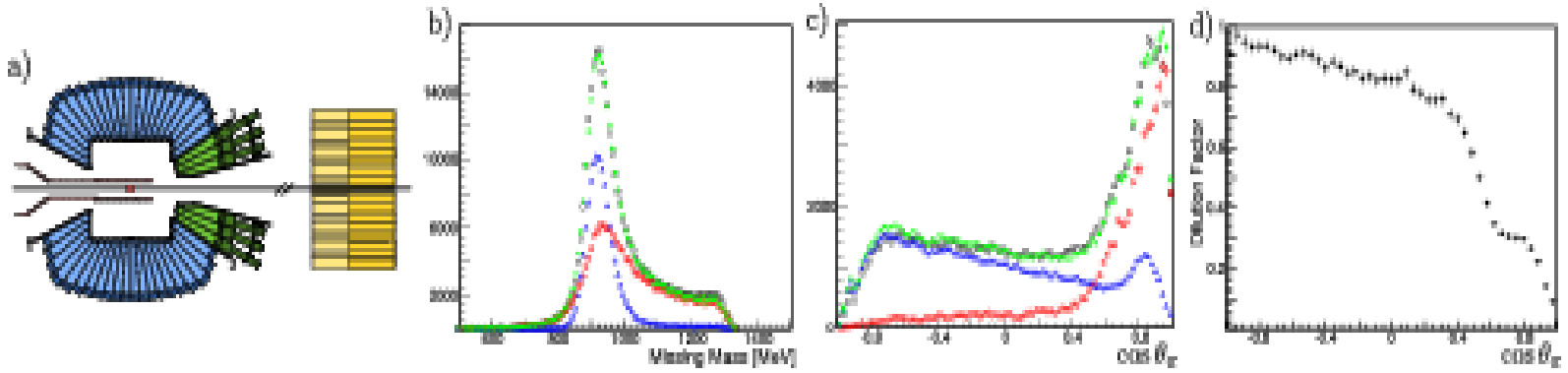

Figure 1. (Color online) a) The central part of the detector system. The CsI(Tl) crystals (blue and green) are read out via wavelength shifters and photodiodes or photomultipliers, BaF_2 crystals (yellow) in forward direction with photomultipliers. b) The missing mass distribution, and (c) the π^0 angular distribution for reaction (1) for an incident photon energy of E_γ = 1000±25 MeV; butanol (□), hydrogen (△), carbon (○), and the sum of hydrogen and carbon data (•). From these distributions, the dilution factor (d) is determined.

Linearly polarized photons were produced by scattering of a 3.3 GeV electron beam off a diamond crystal, whereby maximal polarization of 65% at 950 MeV and 59% at 1150 MeV for second data set where reached. The photons then hit a butanol ($C_4H_{10}O$) target with longitudinally polarized protons, with a mean proton polarization of about 75%. The butanol target was replaced by a hydrogen or carbon target for background studies and for normalization.

The incoming photons may produce a π^0 in the reaction

$$\vec{\gamma}\vec{p} \to p\pi^0. \quad (1)$$

For linearly polarized photons (with polarization p_γ) and protons (with polarization p_T), the number of events N at the polar angle θ_π due to reaction (1) as a function of the azimuthal angle ϕ_π can be written in the form

$$\frac{N(\phi_\pi, \theta_\pi)}{N_0(\theta_\pi)} = 1 - p_\gamma \Sigma_B \cos(2\phi_\pi) + p_\gamma p_T G_B \sin(2\phi_\pi) \quad (2)$$

where N_0 is given by averaging $N(\phi_\pi, \theta_\pi)$ over ϕ_π. The beam asymmetry Σ_B and the observable G_B for the butanol target are related to the corresponding quantities for scattering off free (f) protons Σ, G and bound (b) nucleons by

$$\Sigma_B = \frac{N_0^f \Sigma + N_0^b \Sigma_b}{N_0^f + N_0^b}; \quad G_B = \frac{N_0^f}{N_0^f + N_0^b} \cdot G. \quad (3)$$

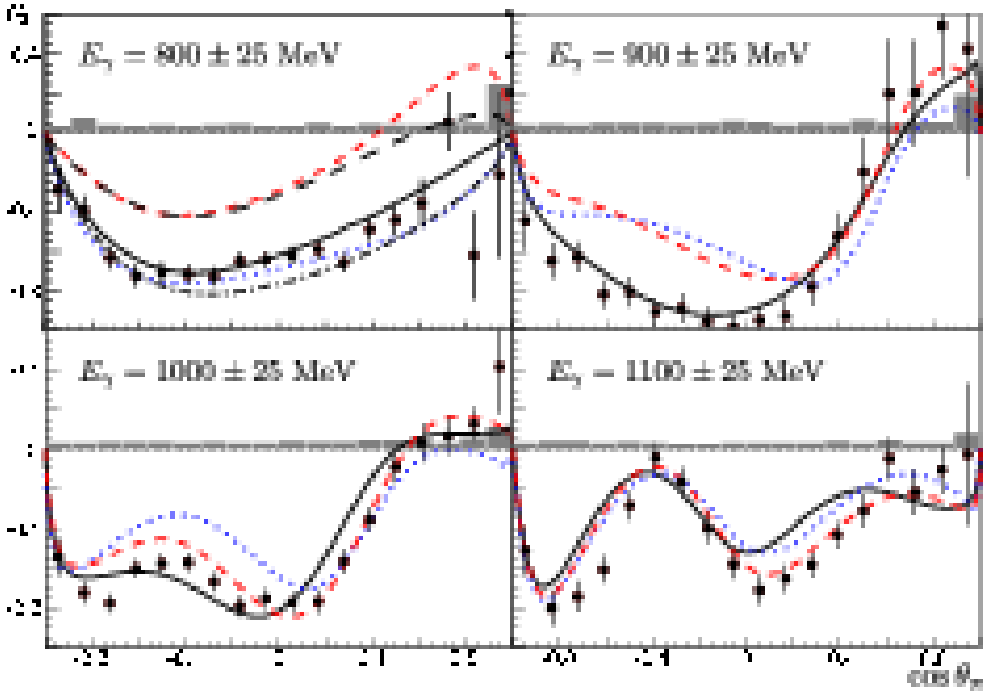

Figure 3. (Color online) The polarization observable G as a function of $\cos\theta_\pi$ from $E_\gamma = 800$ MeV up to $E_\gamma = 1100$ MeV. Systematic errors are shown in gray bars. Curves: see fig. 2.

Solid (black) curve-PWA BnGa; dashed (red) – PWA SAID; dotted (blue)-PWA MAID.

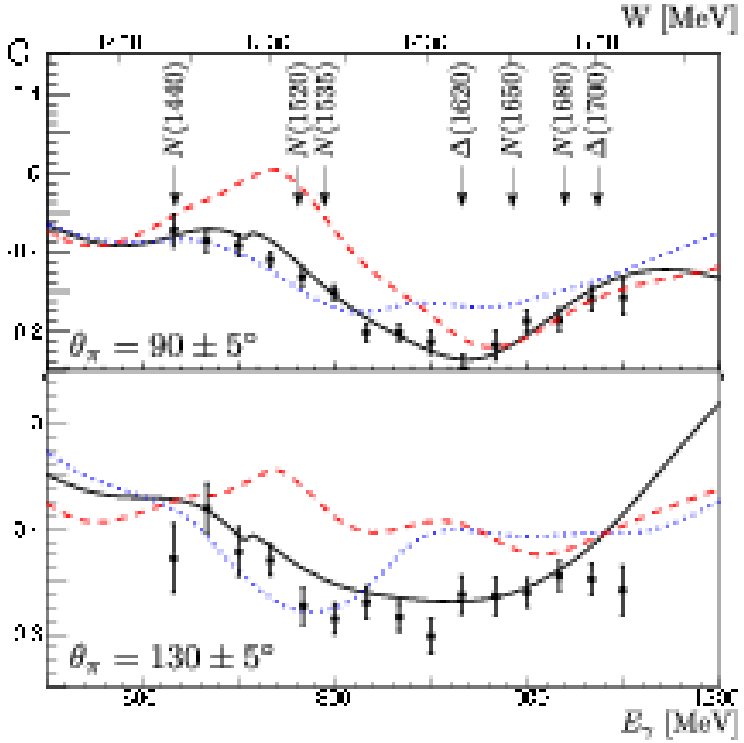

Figure 4. The double-polarization observable G as a function of energy for two selected bins in θ_π. Curves: see fig. 2. For comparison the positions of several resonances are marked.

Transparency ratio in $\gamma A \to \eta' A'$ and the in-medium η' width

Abstract

The photoproduction of η'-mesons off different nuclei has been measured with the CBELSA/TAPS detector system for incident photon energies between 1500 - 2200 MeV. The transparency ratio has been deduced and compared to theoretical calculations describing the propagation of η'-mesons in nuclei. The comparison indicates a width of the η'-meson of the order of $\Gamma = 15 - 25$ MeV at $\rho = \rho_0$ for an average momentum $p_{\eta'} = 1050$ MeV/c, at which the η'-meson is produced in the nuclear rest frame. The inelastic $\eta' N$ cross section is estimated to be 3 - 10 mb. Parameterizing the photoproduction cross section of η'-mesons by $\sigma(A) = \sigma_0 A^\alpha$, a value of $\alpha = 0.84 \pm 0.03$ has been deduced.

Transparency ratio is the ratio of production cross sections per nucleon in different nuclei with respect to the elementary cross section on the nucleon.

The photoproduction cross section A(γ,η')A' in nuclei is not proportional to A for different nuclei, and the deviation from A scaling can be related to the width of the produced particle in the nucleus.

m_η, = 957.78 MeV

Tagged photons with energies of 0.9 - 2.2 GeV, produced via bremsstrahlung at a rate of 8-10 MHz, impinged on a solid target. For the measurements, ^{12}C, ^{40}Ca, ^{93}Nb and ^{208}Pb targets were used with thicknesses of 20, 10, 1, and 0.6 mm, respectively, each corresponding roughly to about 8-10% of a radiation length. The data were collected during two running periods totaling 575 h. Events with η' candidates were selected with suitable multiplicity trigger conditions requiring at least two hits in TAPS or at least one hit in TAPS and two hits in the CB, derived from a fast cluster recognition encoder. A more detailed description of the detector setup and the running conditions can be found in [28, 29].

The η'-mesons were identified via the $\eta' \rightarrow \pi^0\pi^0\eta \rightarrow 6\gamma$ decay channel, which has a branching ratio of 8.1%. For the reconstruction of the η'-meson, only events with at least 6 or 7 neutral hits were selected. Because of the competing channel $\eta \rightarrow \pi^0\pi^0\pi^0 \rightarrow 6\gamma$ with the same final state, this reaction was also reconstructed and the corresponding events were rejected from the further analysis. In addition, only events with one combination of the 6 photons to two photon pairs with mass 110 MeV/c^2 $\leq m_{\gamma\gamma} \leq$ 160 MeV/c^2 close to the π^0 mass and one pair with mass 500 MeV/c^2 $\leq m_{\gamma\gamma} \leq$600 MeV/c^2 close to the η mass were analyzed further.

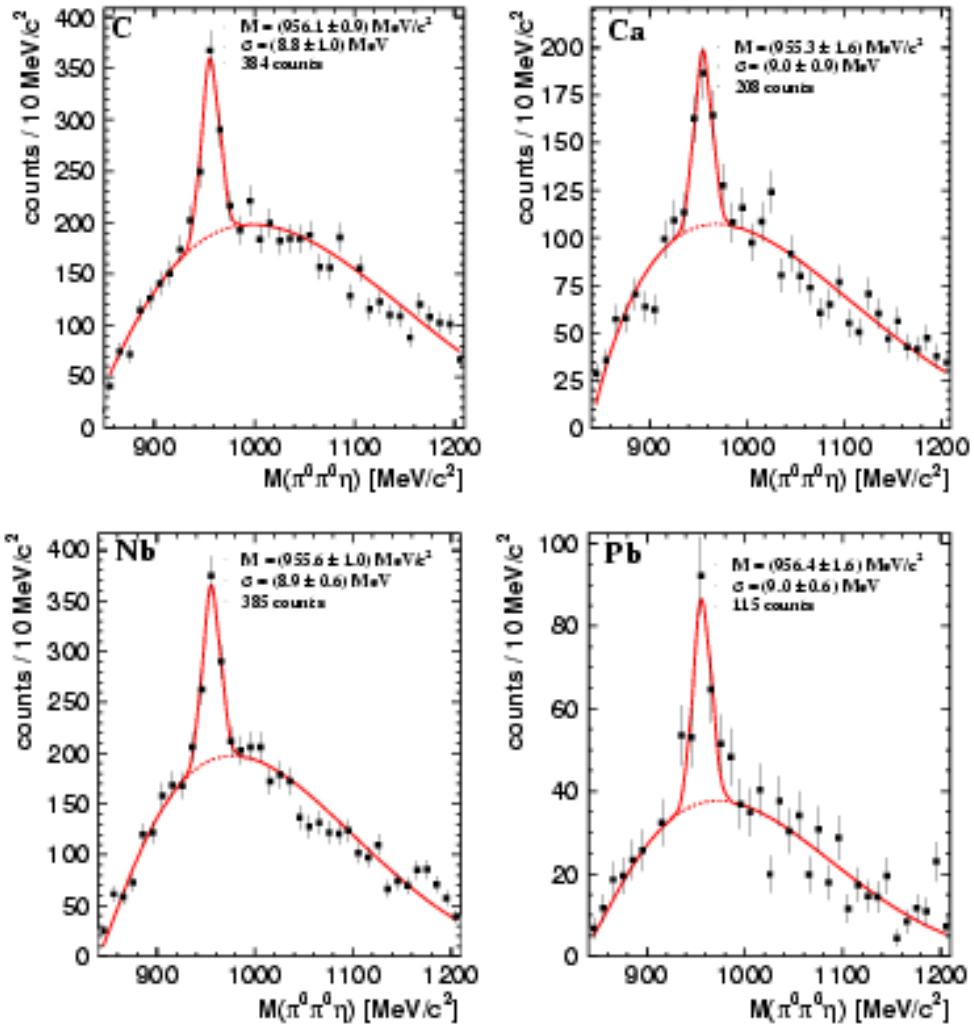

FIG. 1. Invariant mass spectrum of $\pi^0\pi^0\eta$ for ^{12}C, ^{40}Ca, ^{93}Nb and ^{208}Pb targets for the incident photon energy range 1500 - 2200 MeV. The solid curve is a fit to the spectrum. Only statistical errors are given. See text for more details.

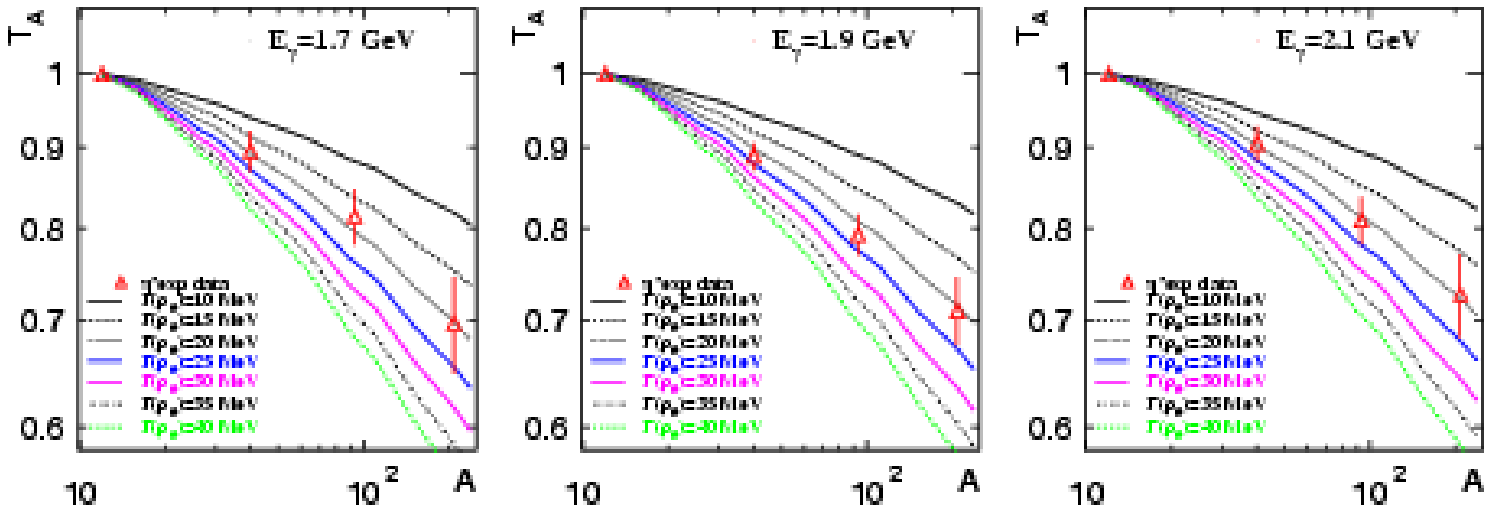

FIG. 2. Transparency ratio relative to that of ^{12}C, $T_A = \tilde{T}_A/\tilde{T}_{12}$, as a function of the nuclear mass number A, for different in-medium widths of the η' at three different incident photon energies. Only statistical errors are shown. The systematic errors are of the order of 20% but tend to partially cancel since cross section ratios are given.

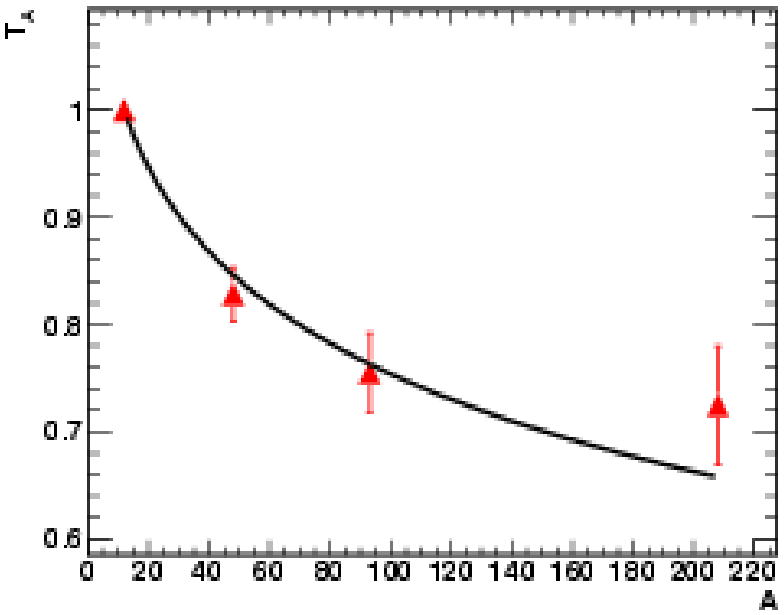

FIG. 3. The transparency ratio for η'-mesons as a function of the nuclear mass number A for the full incident photon energy range of 1500 - 2200 MeV. The solid curve is a fit to the data using expression in Eq.(11).

$$T_A = \frac{\pi R^2}{A\sigma_{\eta' N}} \left\{ 1 + \left(\frac{\lambda}{R}\right) \exp\left[-2\frac{R}{\lambda}\right] + \frac{1}{2}\left(\frac{\lambda}{R}\right)^2 \left(\exp\left[-2\frac{R}{\lambda}\right] - 1 \right) \right\} \qquad (11)$$

where $\lambda = (\rho_0 \sigma_{\eta' N})^{-1}$ is the mean free path of the η'-meson in a nucleus with density ρ_0=0.17 fm^{-3} and radius $R = r_0 A^{1/3}$ with $r_0 = 1.143$ fm.

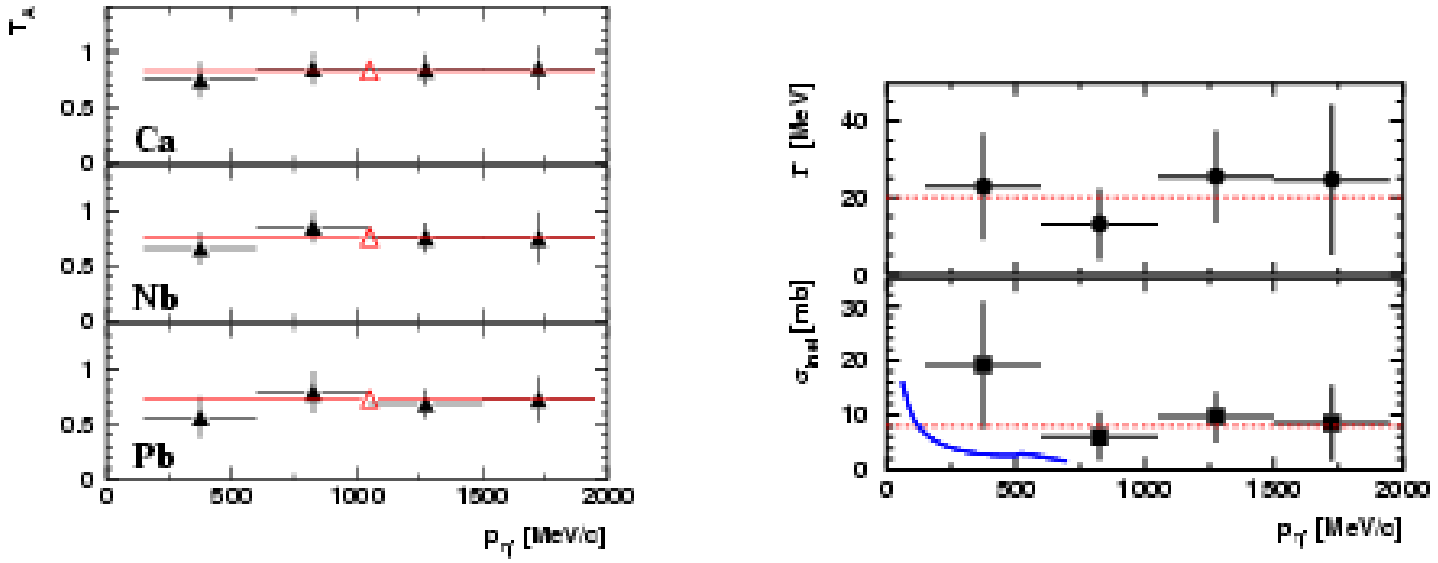

FIG. 5. (Left) Transparency ratio for the η'-meson normalized to C for three different targets: Ca, Nb, and Pb and four bins in η' momentum (full triangles) for the full incident photon energy range from 1500 - 2200 MeV. The open triangles show the values when integrated over all momenta and energies. (Right) The in-medium width (upper panel) and inelastic cross section (lower panel) as a function of the η' momentum. For comparison, the theoretical predictions for σ_{inel} [7] are shown by a blue (solid) curve.

[7] – T.Oset, A.Ramos, Phys. Lett. B 704, 304 (2011)

III. CONCLUSIONS

The transparency ratios for η'-mesons measured for several nuclei deviate sufficiently from unity to allow an extraction of the η' width in the nuclear medium, and an approximate inelastic cross section for $\eta' N$ at energies around $\sqrt{s} \approx 2.0$ GeV. We find $\Gamma \approx 15 - 25$ MeV $\cdot \rho/\rho_0$ roughly, corresponding to an inelastic $\eta' N$ cross section of $\sigma_{\rm inel} \approx$ 6-10 mb. If inelastic and two-body absorption processes were equally strong the inelastic cross section would be reduced to $\sigma_{\rm inel} \approx$ 3-5 mb. Despite of the uncertainties and approximations involved in the determination of $\sigma_{\rm inel}$, this is the first experimental measurement of this cross section. A comparison to photoproduction cross sections and transparency ratios measured for other mesons (π, η, ω) demonstrates the relatively weak interaction of the η'-meson with nuclear matter. Regarding the observability of η' mesic states the measured in-medium width of $\Gamma \approx 15 - 25$ MeV at normal nuclear matter density would require a depth of about 50 MeV or more for the real part of the η' - nucleus optical potential.

Crystal Ball:
- $\mu^{\pm}$: 233 MeV
- $\pi^{\pm}$: 240 MeV
- $K^{\pm}$: 341 MeV
- p: 425 MeV

TAPS:
- $\mu^{\pm}$: 165 MeV
- $\pi^{\pm}$: 180 MeV
- $K^{\pm}$: 280 MeV
- p: 360 MeV

Experimental Setup

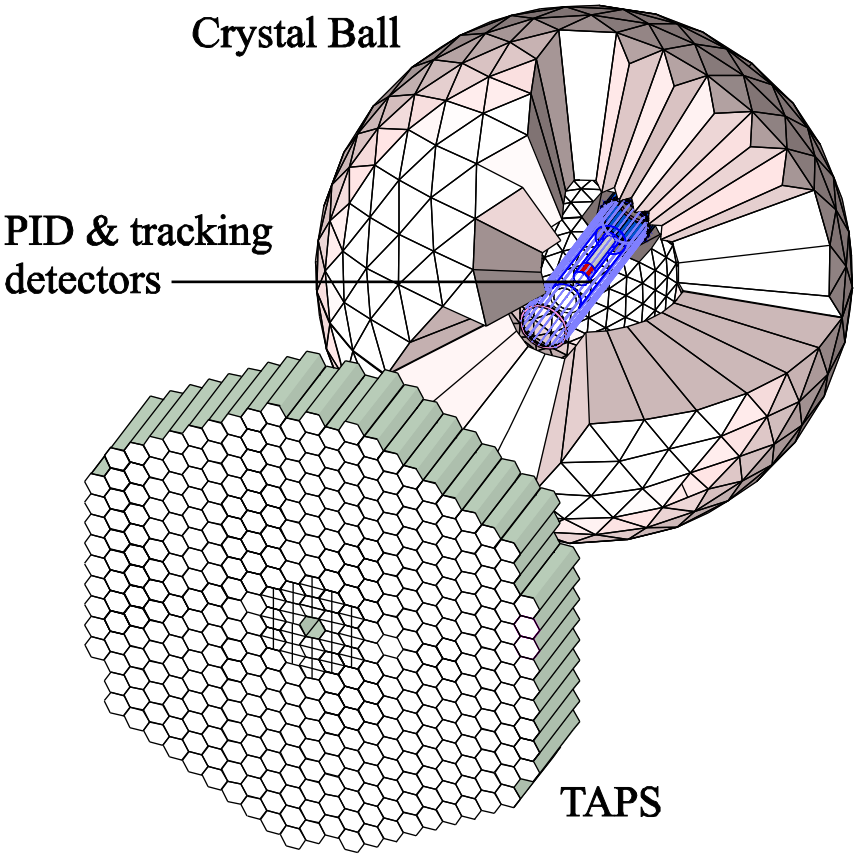

- **Crystal Ball:**
  - 672 NaI crystals about 16 *r.l.*
  - Cover 94% solid angle
  - Angular resolution: σ(φ) is 2-3 degree and σ(Θ) is (2°-3°)/cos(Θ)
  - Energy resolution of about $\Delta E/E=0.02(E[GeV])^{-0.36}$
- **TAPS:**
  - 366 BaF_2 and 72 PbWO crystals
  - Time resolution 160 psec
  - Overall acceptance for EC calorimeter 97%
- **PID:**
  - Barrel of 24, 4 mm thick plastic strips
  - Good time resolution
  - Proton identification using $\Delta E/\Delta x$
- **MWPC:**
  - Two-layers cylindrical chamber
  - Angular resolution 2-3 degrees
  - Minimum material in particular in forward direction

Tagged Photon Beam

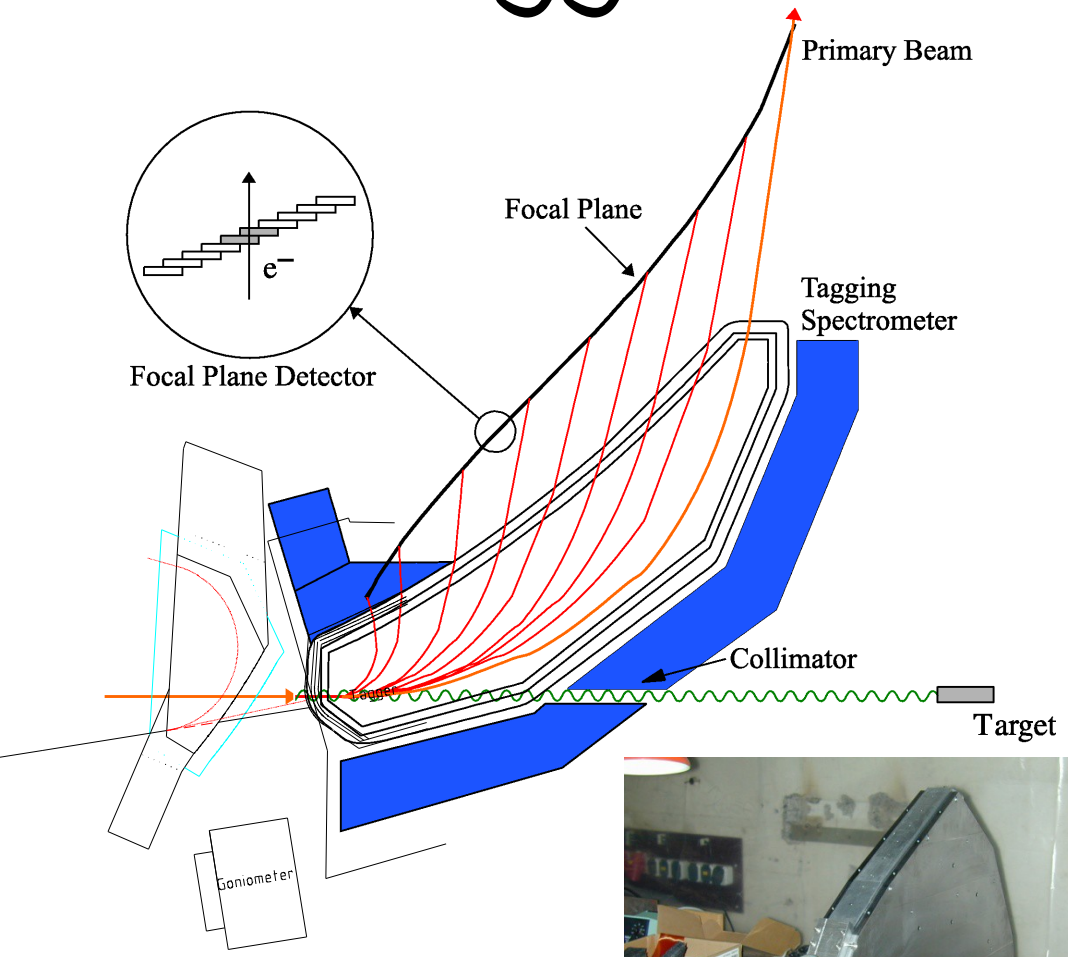

- Maximum electron energy – 1604 MeV
- Maximum energy of tagged photons –
- 1453 MeV with the main tagger,
- and up to 1548 MeV with the end-point tagger
- Energy resolution ~ 4 MeV in the main tagged ladder, ~1 MeV resolution in the microscope

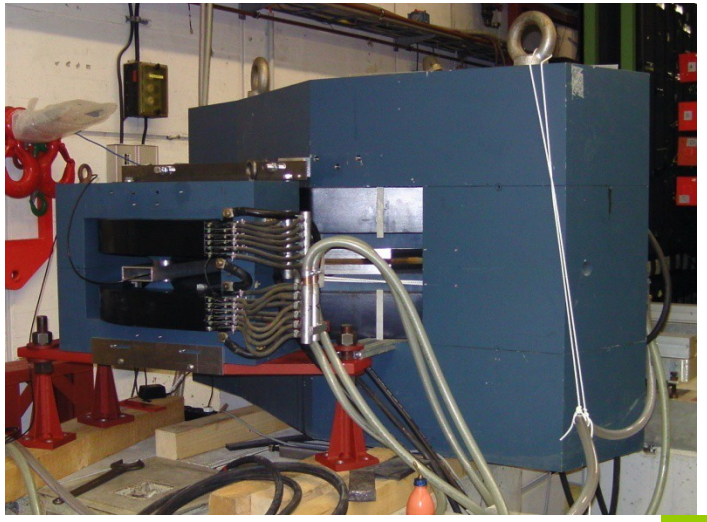

Study of the $\gamma p \to \pi^0\pi^0 p$ reaction with the Crystal Ball/TAPS at the Mainz Microtron

The $\gamma p \to \pi^0\pi^0 p$ reaction has been measured from threshold to 1.4 GeV using the Crystal Ball and TAPS photon spectrometers together with the photon tagging facility at the Mainz Microtron. The experimental results include total and differential cross sections as well as specific angular distributions, which were used to extract partial-wave amplitudes. In particular, the energy region below the $D_{13}(1520)$ resonance was studied.

The present measurement used 855-MeV and 1508-MeV electron beams from the upgraded Mainz Microtron, MAMI-C [31]. The data with the 1508-MeV beam were taken in 2007, and with the 855-MeV beam in 2008. Bremsstrahlung photons, produced by the 1508-MeV electrons in a 10-μm Cu radiator and collimated by a 4-mm-diameter Pb collimator, were incident on a 5-cm-long liquid hydrogen (lH_2) target located in the center of the CB. The energies of the incident photons were measured in the range 617 to 1402 MeV by detecting the post-bremsstrahlung electrons in the Glasgow tagger [32]. With the 855-MeV electron beam, bremsstrahlung photons were produced in a diamond radiator, collimated by a 3-mm-diameter Pb collimator, and incident on a 10-cm-long lH_2 target. In this experiment, the energies of the incident photons were tagged from 84 to 796 MeV. The energy resolution of the tagged photons is mostly defined by the width of the tagger focal plane detectors, and by the electron beam energy. For a beam energy of 1508 MeV, a typical width of a tagger channel was about 4 MeV, and about 2 MeV for a beam energy of 855 MeV. Due to the beam collimation only part of the bremsstrahlung photon flux reached the lH_2 target.

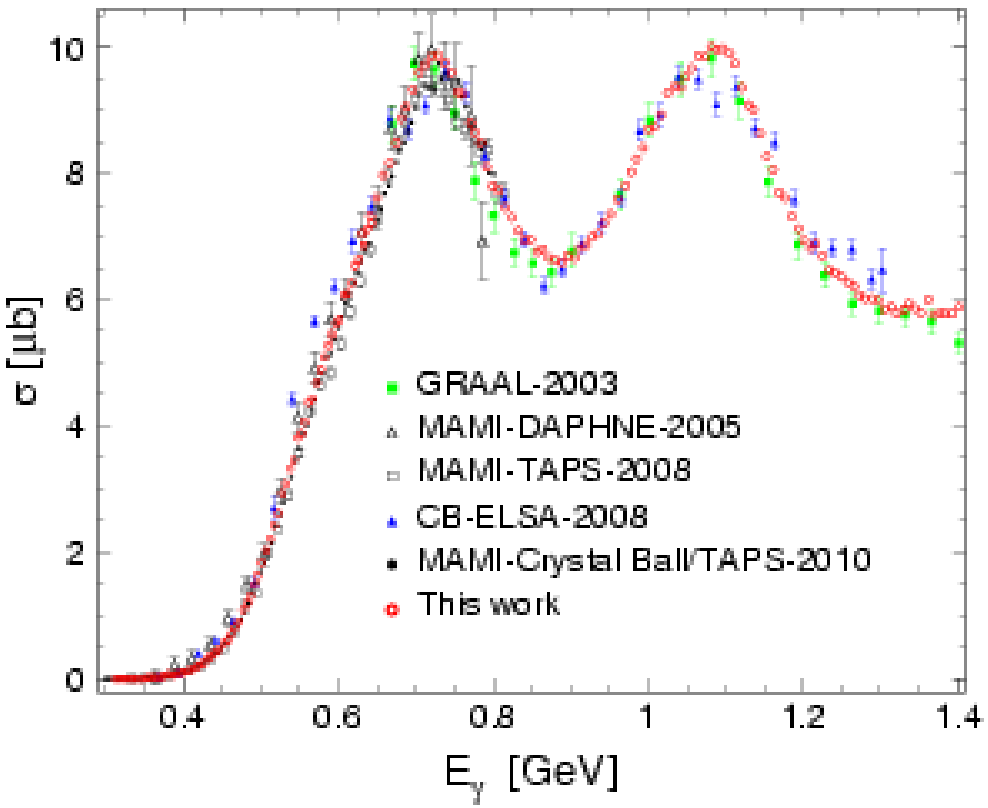

FIG. 1: (Color online) Total cross sections for $\gamma p \to \pi^0\pi^0 p$ are shown as a function of the incident-photon energy. The results obtained in this work are compared to the existing data from GRAAL [6], CB-ELSA [11, 12], DAPHNE [8], TAPS [12], and Crystal Ball/TAPS [40]. Only statistical uncertainties are shown for all data.

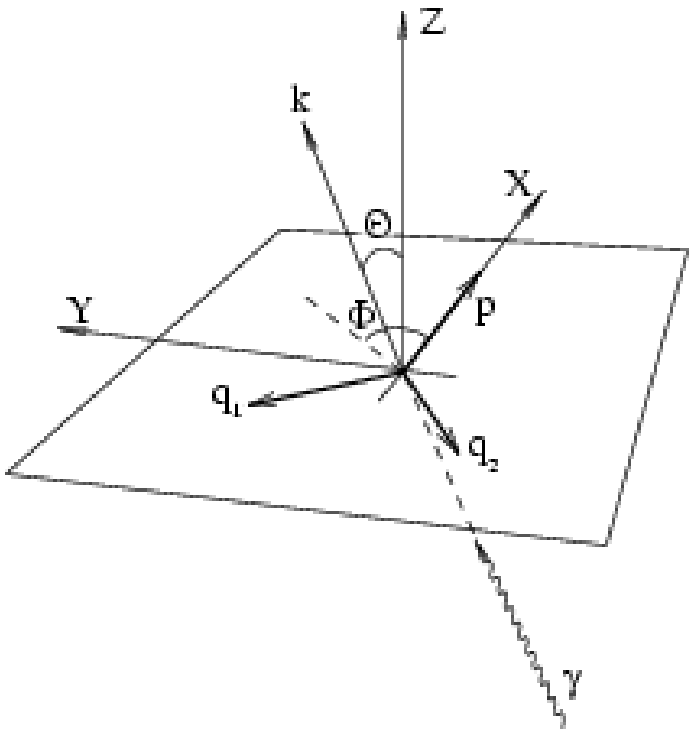

FIG. 3: Definition of the coordinate system used in the present formalism. $\vec{k}$, $\vec{p}$, $\vec{q}_1$, and $\vec{q}_2$ are respectively three-momenta of the incident-photon, out-going proton, two pions in the center of mass system. Axis Z is a normal to the decay plane. Axis X is along $\vec{p}$. Θ and Φ are respectively the polar and azimuthal angles of $\vec{k}$.

$$W(\Theta,\Phi) \equiv \frac{1}{\sigma}\frac{d\sigma}{d\Omega}$$
$$= \sum_{L\geq 0}\sum_{M=-L}^{L}\sqrt{\frac{2J+1}{4\pi}}\,W_{LM}Y_{LM}(\Theta,\Phi)\,, \quad (3)$$

which is expanded over spherical harmonics with $W_{00} = 1$. The coefficients W_{LM} in Eq. (3) are hermitian combinations of the partial-wave amplitudes $t^{JM}_{\nu\mu}$. The corresponding expression was obtained in [26]:

$$W_{LM} = \frac{\pi}{\sigma}\mathcal{K}\int d\omega_1 d\omega_2 \sum_{\nu\mu}\sum_{JJ'M_JM'_J}(-1)^{M+\mu}$$
$$\times C^{LM}_{J'M'_J\,JM_J}C^{L0}_{J'\mu J-\mu}t^{J'M'_J}_{\nu\mu}(\omega_1,\omega_2)^* t^{JM_J}_{\nu\mu}(\omega_1,\omega_2)\,, \quad (4)$$

where $\mathcal{K}$ is an appropriate phase space factor. Formula (3) determines the general structure of an angular distribution in a manner analogous to the expansion of the cross section for single-meson photoproduction in terms of the Legendre polynomials.

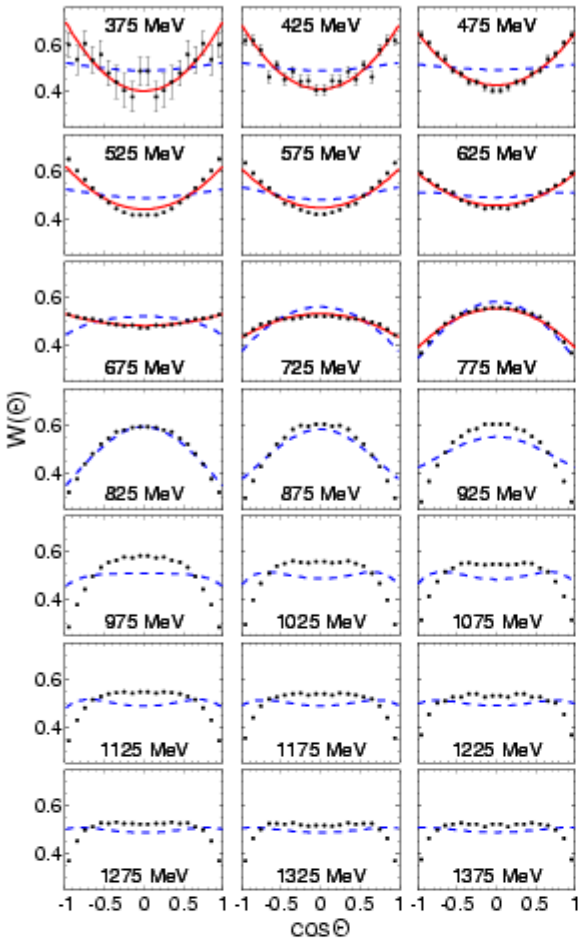

FIG. 4: (Color online) Distribution $W(\Theta) = \int W(\Theta,\Phi)d\Phi$ shown as a function of $\cos\Theta$, where Θ is the polar angle of the incident photon in the coordinate frame presented in Fig. 3. Our experimental results with statistical uncertainties are shown by filled circles. The predictions from the model of Ref. [19] are shown by dashed lines. The results of fitting our data below $E_\gamma = 0.8$ GeV are shown by solid lines. The energy label in each panel indicates the central photon energy for each bin.

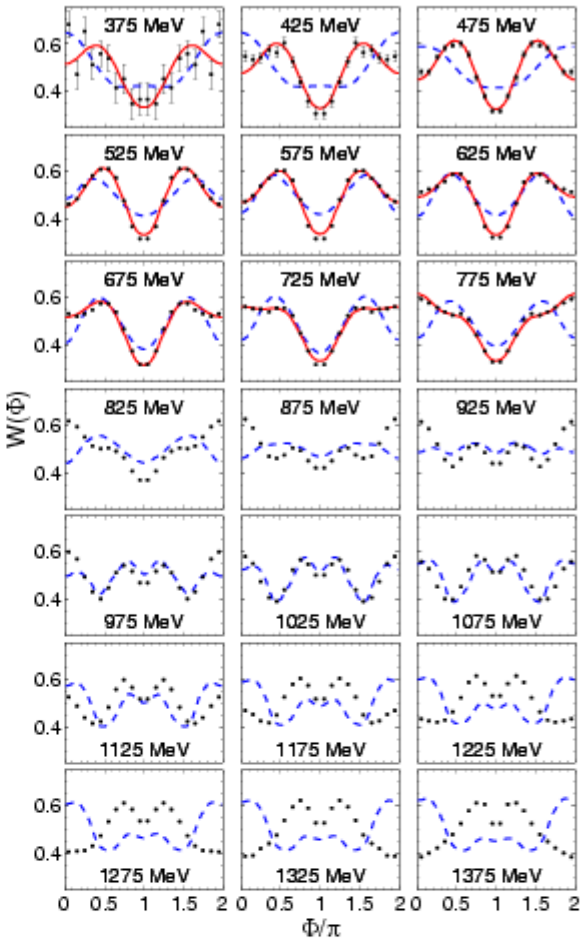

FIG. 5: (Color online) Distribution $W(\Phi) = \pi \int W(\Theta,\Phi)\sin\Theta d\Theta$, where Φ is the azimuthal angle of the incident photon in the coordinate frame presented in Fig. 3. Other notations are the same as in Fig. 4.

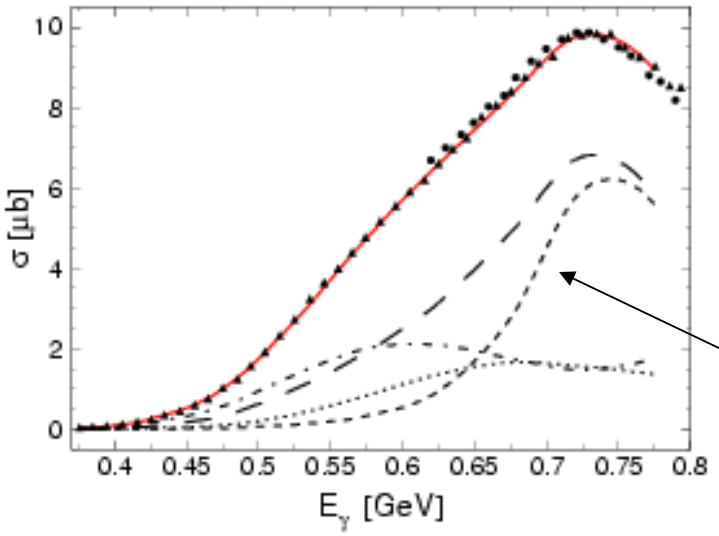

D_{13} (1520)

FIG. 7: (Color online) Total cross section for $\gamma p \to \pi^0\pi^0 p$ as a function of the incident-photon energy. Our experimental results are shown by triangles and circles, respectively for the data with the 855-MeV and 1508-MeV electron beam. Only statistical uncertainties are shown. The fit results for the total cross section are shown by the solid line, and for the $3/2^-$, $3/2^+$, and $1/2^+$ waves by long-dashed, dash-dotted, and dotted lines, respectively. The $D_{13}(1520)$ contribution, calculated from the model of Ref. [19], is shown by the short-dashed line.

[19] A.Fix, H.Arenhoevel , Eur. Rhys. J. A 25, 115 (2005).

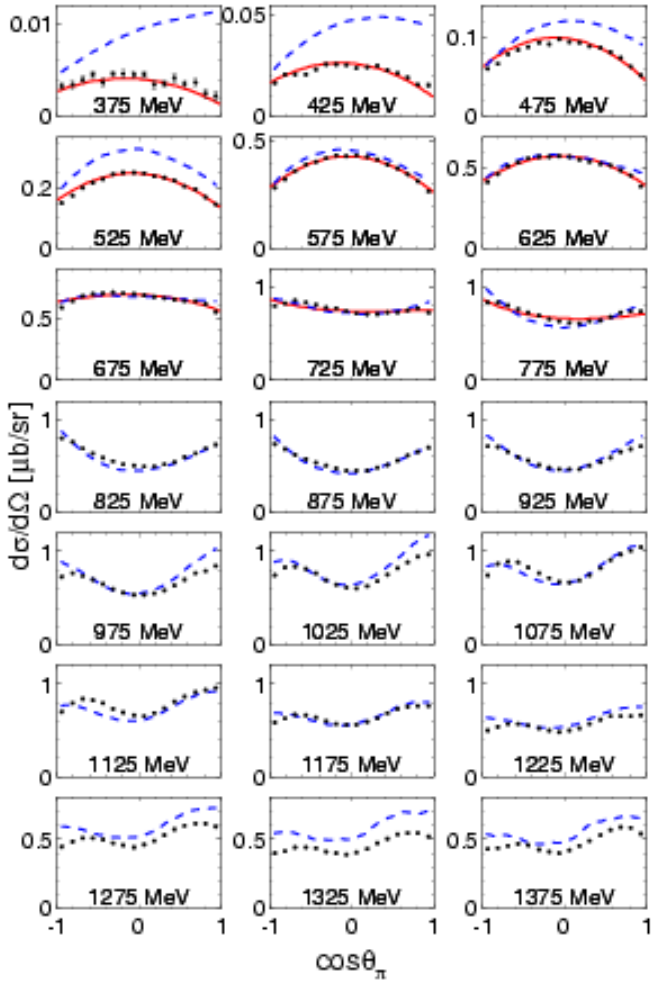

FIG. 8: (Color online) $\gamma p \to \pi^0\pi^0 p$ differential cross sections as a function of the production angle of the outgoing π^0 in the center of mass frame. Since there are two identical pions, each cross section represents the average of two distributions. Our experimental results with statistical uncertainties are shown by filled circles. The predictions from our model are shown by solid lines. The dashed lines result from the Bonn-Gatchina model [11, 12].

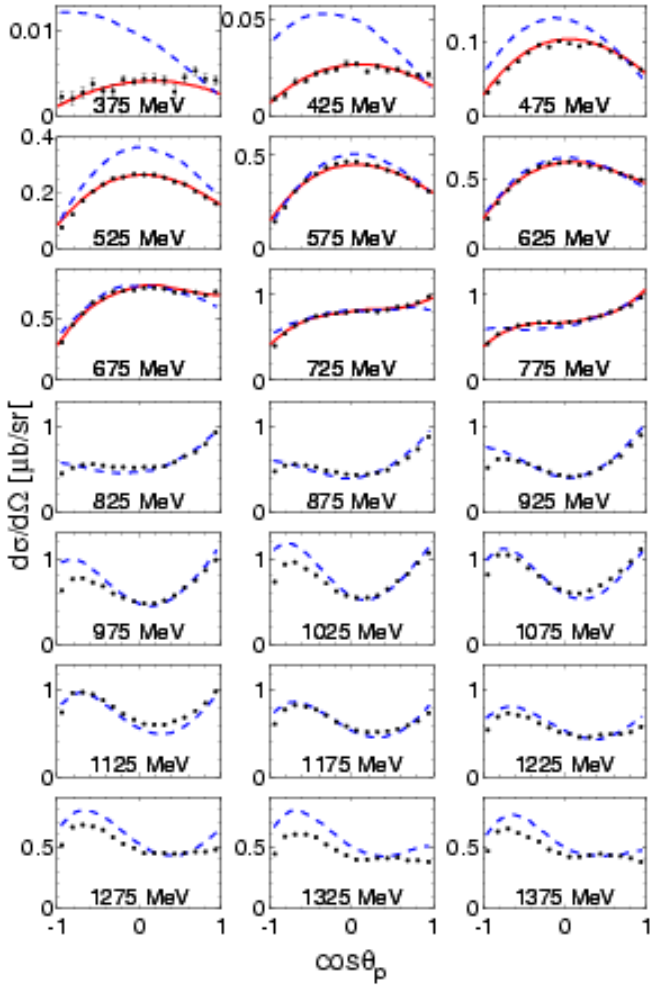

FIG. 9: (Color online) Same as Fig. 8 but for the outgoing proton.

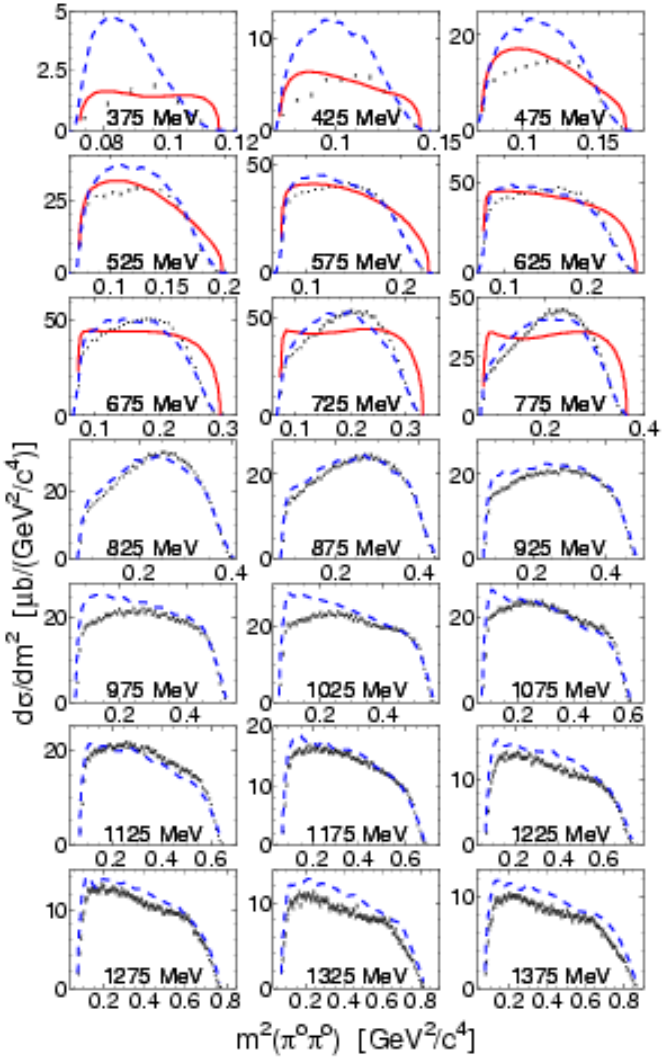

FIG. 10: (Color online) $\gamma p \to \pi^0\pi^0 p$ differential cross sections as a function the invariant mass squared $m^2(\pi^0\pi^0)$. Our experimental results with statistical uncertainties are shown by filled circles. The predictions from our model are shown by solid lines. The dashed lines result from the Bonn-Gatchina model [11, 12].

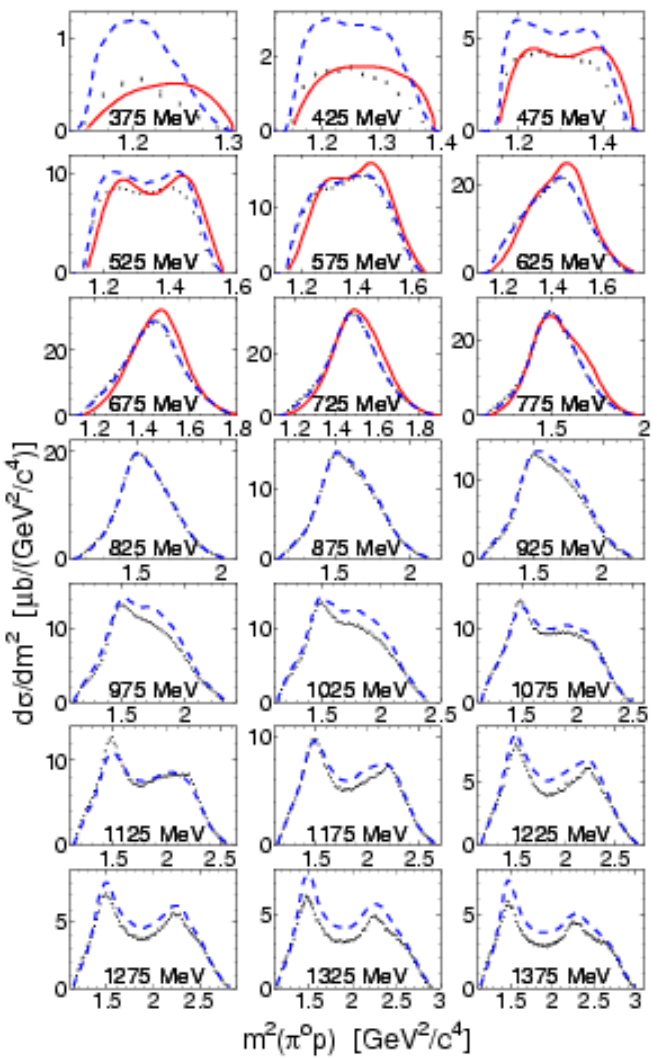

FIG. 11: (Color online) Same as Fig. 10, but for $m^2(\pi^0 p)$. Since there are two identical pions, each cross section represents the average of two distributions.

Our analysis of the energy dependence of W_{LM} showed that a large contribution from the $J = 3/2$ waves is necessary not only in the region of $D_{13}(1520)$ but also at energies below. According to our results, these waves seem to be responsible for an almost linear rise of the $\gamma p \to \pi^0\pi^0 p$ total cross section in the region $E_\gamma = 450 - 725$ MeV. Isobar models with the dominant contribution from $D_{13}(1520)$ and a moderate role for the Roper resonance cannot explain such features in double-π^0 photoproduction. Whether these features are the reflection of a large $J^\pi = 3/2^+$ fraction of $\pi^+\pi^- \to \pi^0\pi^0$ rescattering, or are a consequence of the strong $D_{33}(1700)$ excitation, found in Ref. [12], requires further experimental and theoretical studies.

Coherent photoproduction of η-mesons off ^{3}He - search for η-mesic nuclei

F. Pheron [a], J. Ahrens [b], J.R.M. Annand [c], H.J. Arends [b], K. Bantawa [d], P.A. Bartolome [b], R. Beck [e], V. Bekrenev [f], H. Berghäuser [g], B. Boillat [a], A. Braghieri [h], D. Branford [i], W.J. Briscoe [j], J. Brudvik [k], S. Cherepnya [ℓ], B. Demissie [j], M. Dieterle [a], E.J. Downie [b,c,j], P. Drexler [g], D.I. Glazier [i], E. Heid [b], L.V. Fil'kov [ℓ], D. Hornidge [m], D. Howdle [c], O. Jahn [b], I. Jaegle [a], T.C. Jude [i], V.L. Kashevarov [ℓ,b], I. Keshelashvili [a], R. Kondratiev [n], M. Korolija [o], M. Kotulla [a,g], A. Kulbardis [f], S.P. Kruglov [f], B. Krusche [a], V. Lisin [n], K. Livingston [c], I.J.D. MacGregor [c], Y. Maghrbi [a], J. Mancell [c], D.M. Manley [d], Z. Marinides [j], M. Martinez [b], J.C. McGeorge [c], E. McNicoll [c], D. Mekterovic [o], V. Metag [g], S. Micanovic [o], D.G. Middleton [m], A. Mushkarenkov [h], B.M.K. Nefkens [k], A. Nikolaev [e], R. Novotny [g], M. Oberle [a], M. Ostrick [b], B. Oussena [b,j], P. Pedroni [h], A. Polonski [n], S.N. Prakhov [k], J. Robinson [c], G. Rosner [c], T. Rostomyan [a,h], S. Schumann [b], M.H. Sikora [i], D.I. Sober [p], A. Starostin [k], I. Supek [o], M. Thiel [g], A. Thomas [b], M. Unverzagt [b], D.P. Watts [i], D. Werthmüller [a], L. Witthauer [a], F. Zehr [a]

Abstract

Coherent photoproduction of η-mesons off ^{3}He, i.e. the reaction $\gamma^3\mathrm{He} \to \eta^3\mathrm{He}$, has been investigated in the near-threshold region. The experiment was performed at the Glasgow tagged photon facility of the Mainz MAMI accelerator with the combined Crystal Ball - TAPS detector. Angular distributions and the total cross section were measured using the $\eta \to \gamma\gamma$ and $\eta \to 3\pi^0 \to 6\gamma$ decay channels. The observed extremely sharp rise of the cross section at threshold and the behavior of the angular distributions are evidence for a strong η^3He final state interaction, pointing to the existence of a resonant state. The search for further evidence of this state in the excitation function of π^0-proton back-to-back emission in the $\gamma^3\mathrm{He} \to \pi^0 pX$ reaction revealed a very complicated structure of the background and could not support previous conclusions.

2. Experiment and analysis

The experiment was performed at the tagged photon beam of the Mainz MAMI accelerator [50,51]. The electron beam of 1508 MeV was used to produce bremsstrahlung photons in a copper radiator of 10μm thickness, which were tagged with the upgraded Glasgow magnetic spectrometer [52–54] for photon energies from 0.45 GeV to 1.4 GeV. The typical bin width for the photon beam energy (4 MeV) is defined by the geometrical size of the plastic scintillators in the focal plane detector of the tagger. The intrinsic resolution of the magnetic spectrometer is better by more than an order of magnitude. The size of the tagged photon beam spot on the target was restricted by a 3 mm diameter collimator placed downstream from the radiator foil. The target was a mylar cylinder of 3.0 cm diameter and 5.08 cm length filled with liquid ^{3}He at a temperature of 2.6 K. The corresponding target density was 0.073 nuclei/barn.

The reaction products were detected with an electromagnetic calorimeter combining the Crystal Ball detector (CB) [55] made of 672 NaI crystals with 384 BaF_2 crystals from the TAPS detector [56,57], configured as a forward wall. The Crystal Ball was equipped with an additional **P**article **I**dentification **D**etector (PID) [58] for the identification of charged particles

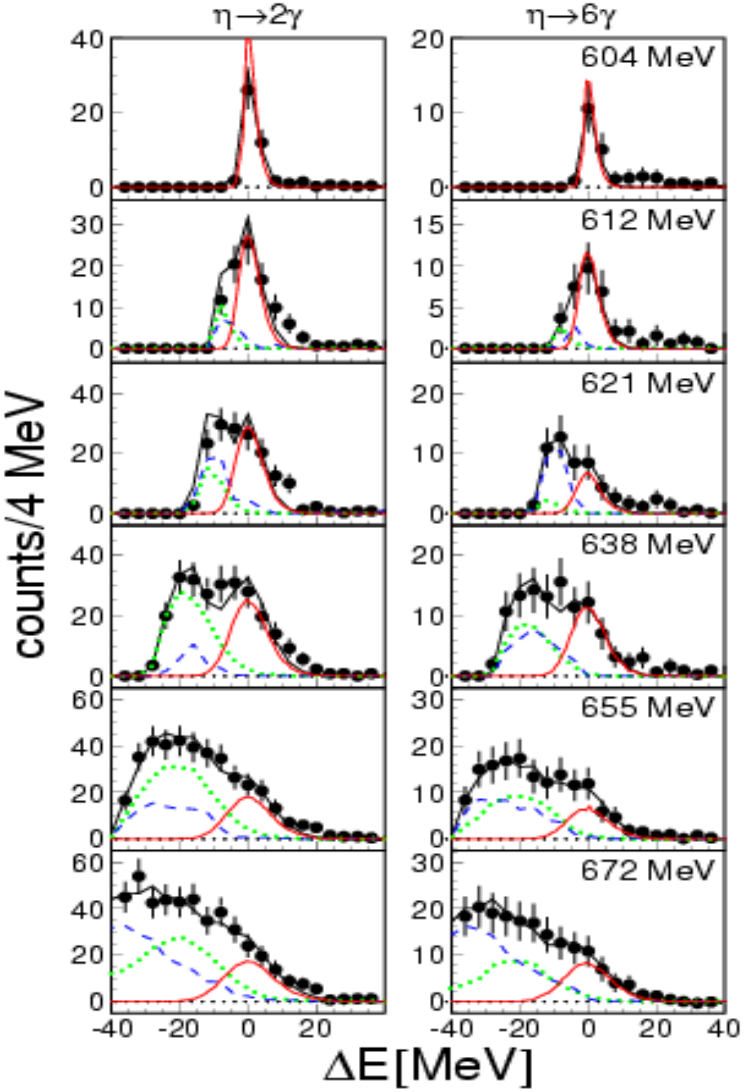

Fig. 1. Missing energy spectra for the $\gamma^3\mathrm{He} \to \eta^3\mathrm{He}$ reaction for the two-photon and $3\pi^0$ decay modes for different ranges of incident photon energy. Black dots: experiment. Curves: Monte Carlo simulations. Solid (red): coherent contribution, dashed (blue): recoil taken by quasi-free nucleon, dotted (green): recoil taken by di-nucleon, solid (black) sum of all.

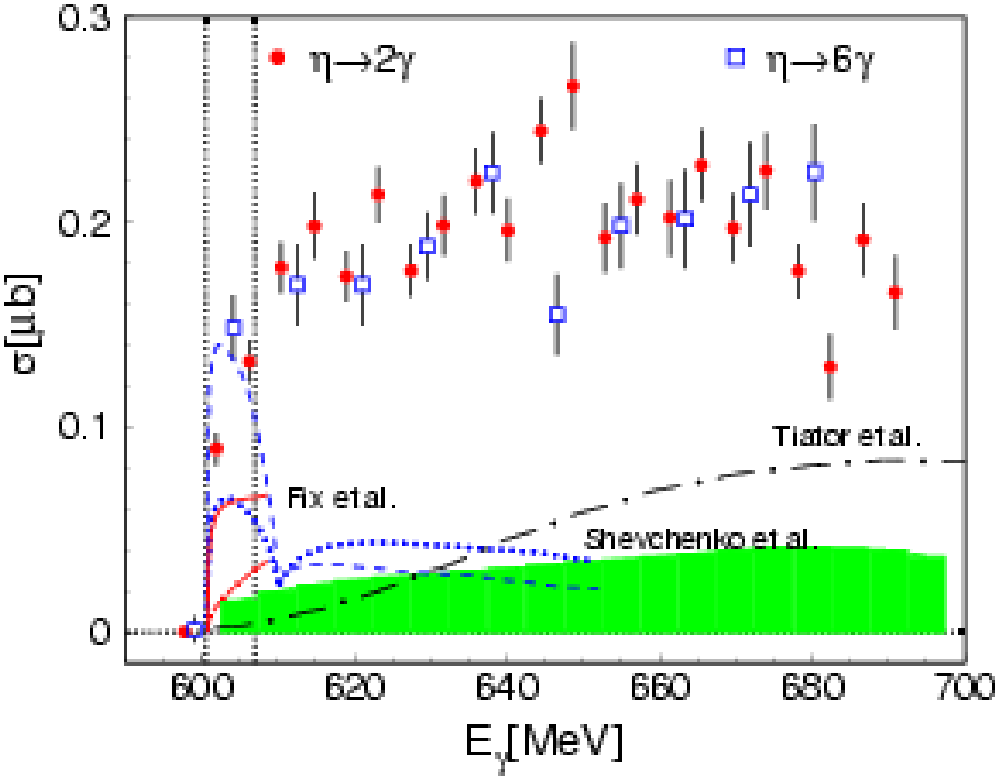

Fig. 2. Total cross section for the γ^3He$\rightarrow\eta^3$He reaction from $\eta \rightarrow 2\gamma$ and $\eta \rightarrow 6\gamma$ decays. The shaded band at the bottom indicates the systematic uncertainty. The two vertical lines indicate coherent and breakup threshold. Theory curves: (blue) dotted and dashed from Shevchenko et al. [66] for two different versions of elastic ηN scattering, (red) solid (dash-dotted): Fix and Arenhövel [65] full model (plane wave), (black) long dash-dotted: Tiator et al. [64].

$\eta - 2\gamma$ (39.31 %) ; $\eta - 3\pi^0$ (32.57 %) [Rev. of Part. Phys.]

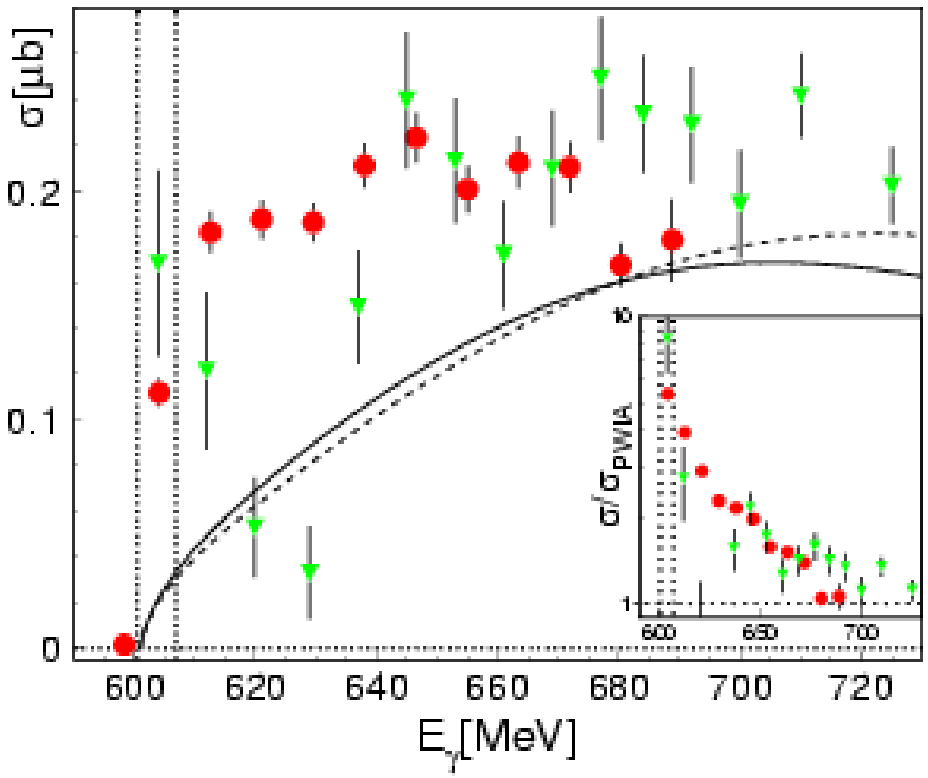

Fig. 3. Total cross section for γ^3He$\to\eta^3$He (averaged over 2γ and $3\pi^0$ decays) (red dots) compared to previous data [47] (green triangles). Solid (dashed) curves: PWIA with realistic (isotropic) angular distribution for $\gamma n \to n\eta$ (see text). The present data are binned in the same way as the angular distributions in Fig. 4 (bin width $\approx$8 MeV). Insert: ratio of measured and PWIA cross sections.

4. Summary and conclusions

Coherent photoproduction of η-mesons off ^{3}He has been measured with much improved statistical quality compared to the pilot experiment of Pfeiffer et al. [47]. The total cross section rises sharply between the coherent and breakup thresholds. Compared to a PWIA, which is in fair agreement with the data in the S_{11} peak, the threshold values are enhanced by nearly one order of magnitude. This is very different e.g. from the behavior of coherent η photoproduction off the deuteron, which is in reasonable agreement with PWIA [15]. The angular distributions at threshold are almost isotropic, and are unlike the forward peaked distributions expected to result from the form factor behavior. This result is similar to that previously observed for the hadron induced reactions $pd \to \eta^3$He [37] and $dp \to \eta^3$He [38–40]. This independence from the initial state is strong evidence for dominant η-nucleus interaction effects, related to a resonant state in the vicinity of the η production threshold.

Determination of the η mass with the Crystal Ball at MAMI-B

The Crystal Ball at MAMI, TAPS and A2 Collaborations

A. Nikolaev[1], P. Aguar-Bartolomé[2], J. Ahrens[2], J. R. M. Annand[3], H. J. Arends[2], R. Beck[1,*], V. Bekrenev[4], B. Boillat[5], A. Braghieri[6], D. Branford[7], W. J. Briscoe[8], J. W. Brudvik[9], S. Cherepnya[10], R. Codling[3], M. Dehn[2], E. J. Downie[3], L. V. Fil'kov[10], D. I. Glazier[7], R. Gregor[11], E. Heid[2], D. Hornidge[12], O. Jahn[2], A. Jankowiak[2], K.-H. Kaiser[2], V. L. Kashevarov[10], R. Kondratiev[13], M. Korolija[14], M. Kotulla[11], D. Krambrich[2], B. Krusche[5], M. Lang[1], V. Lisin[13], K. Livingston[3], U. Ludwig-Mertin[2], S. Lugert[11], I. J. D. MacGregor[3], D. M. Manley[15], M. Martinez-Fabregate[2], J. C. McGeorge[3], D. Mekterovic[14], V. Metag[11], B. M. K. Nefkens[9], R. Novotny[11], R. O. Owens[3], P. Pedroni[6], A. Polonski[13], S. N. Prakhov[9], J. W. Price[9], A. Reiter[2,3], G. Rosner[3], M. Rost[2], T. Rostomyan[5,6], S. Schumann[1,2], D. Sober[16], A. Starostin[9], I. Supek[14], C. M. Tarbert[7], A. Thomas[2], M. Unverzagt[1,2], Th. Walcher[2], D. P. Watts[7], F. Zehr[5]

Abstract A new precise determination of the η meson mass is presented. It is based on a measurement of the threshold for the $\gamma p \to p\eta$ reaction using the tagger focal-plane microscope detector at the MAMI-B facility in Mainz. The tagger microscope has a higher energy resolution than the standard tagging spectrometer and, hence, allowed an improvement in the accuracy compared to the previous η mass measurement at MAMI-B. The result $m_\eta = (547.851 \pm 0.031_{\text{stat.}} \pm 0.062_{\text{syst.}})$ MeV agrees very well with the precise values of the NA48, KLOE and CLEO collaborations and deviates by about 5σ from the smaller, but also very precise value obtained by the GEM collaboration at COSY.

Rev. of Part. Phys. (2010) $m_\eta = 547.853$ +/ - 0.024 MeV

ЛМФ 2012 (гамма-нуклон)